OF THE CALIFORNIA DENTAL ASSOCIATION

Journal

DECEMBER 2007

Salivary Assay

CBCT Images

Microarray Analysis

OF THE CALIFORNIA DENTAL ASSOCIATION
Journal
CDA Journal
Volume 35, Number 12
DECEMBER 2007

DEPARTMENTS

FEATURES

CDA JOURNAL, VOL 35, Nº12

You Gotta Have Heart

ALAN L. FELSENFELD, DDS

It would not be a HIPAA violation if I shared a personal health problem with you, or at least I don't think that it would be. As a child, I had rheumatic fever and remember the time spent in bed, and the antibiotics mixed in applesauce that I took (or sometimes spit out when my parents were not looking). A lingering heart murmur, which is heard variably depending on the physician and day, is the residual defect that accompanied this childhood malady. It was clear I required antibiotics prior to dental procedures that involved potential for bleeding and bacteremia.

As I grew, I followed the regimens of the American Heart Association and premedicated myself for cleanings, extractions and sometimes fillings, even before I became a dentist and had better understanding of the need to do so. The antibiotic selections and doses have changed significantly in the past 50 years. The most recent recommendations have radically altered the way we need to treat our patients, and ourselves, based on the best science available.

I remember fondly, well, not so fondly, my classmates practicing intramuscular injections into normally clothed parts of me (what was I thinking?) prior to a dental cleaning. With relief, and with greater need for compliance, came the two days before and two days after oral medication sequence that was less painful but more difficult to follow. As clinical experience matured, the regimens were made simpler by easing the requirements for oral penicillin to one hour prior to a procedure followed by two days after for additional protection. Ultimately, the medication of choice changed to amoxicillin with one dose of 3 grams prior to dental treatment then one-half of the initial dose six hours later. The iteration prior to the current standards, called for 2 grams (still four large capsules that are difficult to swallow but improvement nonetheless) with no follow-up dosing required.

Most patients do not need antibiotic prophylaxis to prevent cardiac infection.

What should be obvious from my personal history is the gradual but definite trend to decreasing doses of antibiotics required to provide prophylaxis against infective endocarditis in a subset of patients and procedures that increase risk. This, too, causes some confusion. The categorization of who is at risk and for which procedures in the previous guidelines became complex. The most recent publication supports that which might have been obvious from the start—most patients do not need antibiotic prophylaxis to prevent cardiac infection. New protocols recommend that only the highest-risk patients need medication prior to procedures that are likely to produce bacterial loading of the bloodstream. So why did I need so many antibiotics for so long when there is no evidence to show that it was efficacious?

Patients are confused about the new regimens. It is difficult to educate a patient, who is used to taking antibiotics prior to dental procedures, that this may not always be necessary. The fear of patients contracting a cardiac infection is difficult to overcome by dentists' counseling since they have been conditioned to take the medication. The comfort level of our colleagues in discussing this with their patients also may be variable.

Physicians are confused about the new regimens. While generally it is not necessary to discuss premedication by AHA protocols for those patients who require such, some of our colleagues consult regularly about this with the treating physicians. On occasions when I have the opportunity to speak with internists and cardiologists about their patients, I have been surprised at their reactions. Some have told me that they have never accepted the established protocols and used what they believed to be better drug sequences with their patients. Others have proffered they did not accept the new guidelines and still recommend premedication for invasive dental procedures. Rumor is, and it is strictly rumor at this

time, that a significant group of cardiologists is unhappy with the guidelines as written and that the occasional overmedication of some patients was preferable to allowing even a small segment of patients to be at risk for a potentially fatal disease. Regrettably, there are a handful of physicians who did not even know the recommendations have changed.

What's a dentist to do? How do we deal with the confusion surrounding what appears to be a radical departure from what has been comfortable for so long? We need to go with the science. While the American Heart Association states their recommendations are only guidelines, they become de facto standards of care. Anyone who has spent any time analyzing the literature and evaluating scientific evidence understands that a literature review or consensus conference of panels of experts inherently is not scientific validation of fact. But when that is the best evidence that is available or when the retrospective studies support the latest approaches to the use of medications, it is the best that we have and has value.

As a profession, we need to be vigilant in our understanding of contemporary treatment protocols for patients with heart problems meriting antibiotic prophylaxis. The indiscriminate use of antibiotics—something that dentistry tends to do with some regularity—is not of value to our patients. We need to be aware of indications and contraindications for antibiotic usage under all circumstances and not be spurious in the use of potentially harmful drugs. This is a difficult concept for many of us to accept.

So where does that leave me? I had my teeth cleaned last week. I did not premedicate. Free at last. ■■■■

Address comments, letters, and questions to the editor at alan.felsenfeld@cda.org.

CDA JOURNAL, VOL 35, Nº12

The *Journal* Can Do Better

I read with unease the recent article by Gregori M. Kurtzman, DDS, in the September issue of the *Journal of the California Dental Association* titled "Simplifying Endodontics With EndoSequence Rotary Instrumentation." While I commend the disclaimer at the onset of the manuscript describing Dr. Kurtzman's participation in the promotion of the EndoSequence file, I have some troubling concerns.

This manuscript is listed under "Features" in the Table of Contents. I am well aware of a history of the *Journal* of labeling manuscripts "opinion" when reviewers or the editorial board considered manuscripts to be anecdotal or unsupported by evidence. My criticism is neither with Dr. Kurtzman for his opinions nor the EndoSequence filing system for its value. My concern is with the *Journal* for publishing such a transparent piece of commercial advertising without identifying it as such. The manuscript makes numerous claims for the superiority of this file, none of them substantiated by research or any cited evidence. The two citations listed at the end of the article are publications by individuals who are also identified with sales of the EndoSequence system.

There are numerous claims in the article that promote the use of this system while offering negative comparisons in the behavior of other systems. This is done without any citation to research. There is nothing offered that might allow the reader to critically assess the arguments and statements put forth. A single example of the overstatements inherent in an opinion article of this kind is the argument made for the superiority of electroplating of ground nickel-titanium rotary instruments in preventing stress fractures. This design feature has so far been equivocal in its benefits and as recently as September, the *Journal of Endodontics* published "A Scanning Electron Microscopy Evaluation of Microfractures, Deformation, and Separation in EndoSequence and Profile Nickel-Titanium Rotary Files Using an Extracted Molar Tooth Model." This research by Herold, Johnson and Wenckus at the University of Illinois, Chicago, states that "unique file design and electropolishing did not inhibit the development of microfractures in EndoSequence nickel-titanium rotary files" and in this single study better performance was demonstrated by a competing file system. The danger here is that this evidence is from a single study and requires corroboration by other researchers.

I am not arguing the positives or negatives of any file system. I am arguing for more quality control in the jury system of our *Journal* and recommending a system similar to that utilized by many current journals, which categorize articles by content (e.g., research, clinical case report, opinion, etc.). How can our readership make informed decisions about what is in the best interest of their patients and practices if they are not adequately informed by their resources of the vetting process to publication or where an article stands in the hierarchy of evidence?

The *Journal of the California Dental Association* can do a lot better than this.

ALAN H. GLUSKIN, DDS
Professor and chair, Endodontics
University of the Pacific Arthur A. Dugoni School of Dentistry, San Francisco

Parental Responsibility Lacking

It was with interest that I read the article "Disparities in Children's Oral Health and Access to Care" in the September issue of the *Journal of the California Dental Association*.

Many of the points the author, Ms. Lesa Paige Bentley, makes are poignant as she addresses the need to eliminate barriers to care. In my practice we choose to treat children with Medi-Cal. From observations at this office, she misses one significant barrier: lack of parental responsibility.

In the Medi-Cal system, most of the patients have no out-of-pocket expenses for treatment. All they have to do is show up. For whatever reason the patients who invariably are dismissed from my practice due to lack of follow-up are dismissed due to parental indifference, carelessness, and irresponsibility. Unfortunately, the state cannot legislate parents to be more responsible. What is most unfair about this is that children suffer. If parents would become more responsible, many of the health care issues facing our children would disappear: childhood diabetes, obesity, at-risk behaviors, etc.

In order to make a significant change in children's health issues, parents, not insurance companies (whose primary goal it is to improve the financial bottom line of the company—not provide health benefits for their policy holders) nor state agencies, must make wise, responsible decisions for both treatment and prevention of all health related issues.

BRIAN W. DUDAR, DDS
Paradise, Calif.

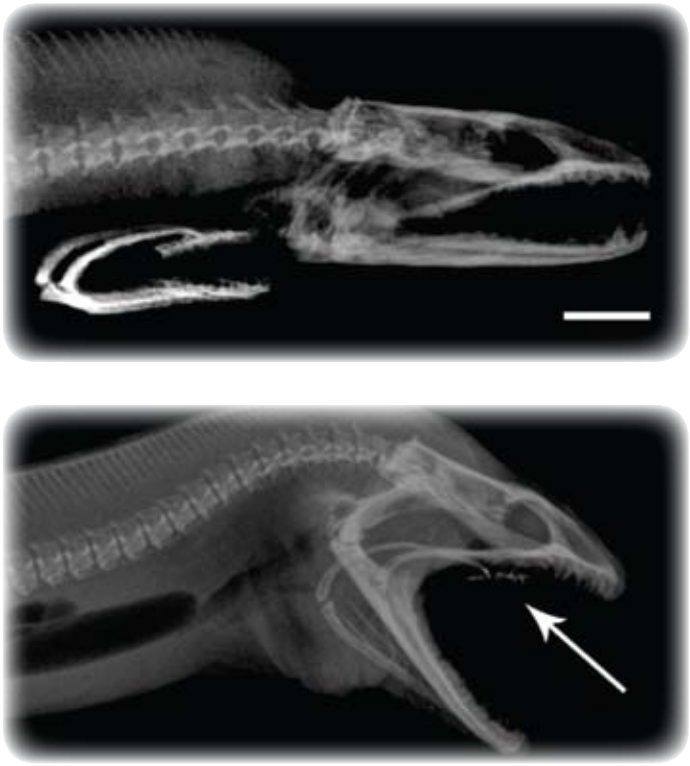

These X-rays show a moray eel's head and jaws: the top with the mouth slightly open and the bottom with the mouth wide open, revealing the second set of jaws. (X-ray courtesy of Candi Stafford and Rita Mehta/UC Davis)

There's More to Morays

BY PATTY REYES

In what is likely the creepiest discovery made this year, scientists at the University of California, Davis, have learned that moray eels possess mobile jaw No. 2 just behind their skull.

After the eel's main jaws clenches its meal, it releases it momentarily and a nimble set of curved, second choppers propels forward and pulls the food back to gulp it down. Only fractions of a second are all it takes for this process. Luckily for the prey, the second mouth cannot protract afar the first. However, the ability to deliver not one but two bites is still a potent weapon in helping the eels feed, said Rita Mehta and Peter Wainwright of UCD who made the discovery, according to various news reports.

"This is really an amazing innovation for feeding behavior for fishes in general," said Mehta, a postdoctoral researcher in the Section of Evolution and Ecology at

CONTINUES ON 837

Zimmer One-Piece Implant Now Available in 3.0 mm Angled for U.S.

Zimmer Dental Inc. is pleased to introduce the 3.0 mm diameter, 17-degree angled Zimmer One-Piece Implant to the U.S. market. All diameters (3.0, 3.7, and 4.7 mm) are now available globally in straight and angled designs. The latest angled Zimmer One-Piece Implant uniquely addresses clinician and patient needs in very challenging anterior areas where space is limited and an angled abutment is required. For more information, call (800) 854-7019 or go to www.zimmerdental.com.

Gingival Cell Trauma May Be Beneficial

Tearing open gingival cells when toothbrushing may help keep gingivae healthy, say researchers in the August issue of *Journal of Dental Research*.

At the Medical College of Georgia in Augusta, researchers injected a fluorescent dye that can only get into torn cells in rats' blood streams. They then brushed the rats' gums, teeth, and tongues with a modified electric toothbrush.

"We saw lots of bright cells," said study co-author Katsuya Miyake, PhD, professor, School of Medicine, and co-director of the college's Cell Imaging Core Facility.

They also found that even using the toothbrush with gentle force could tear holes in the epithelial cells lining the gingivae and tongue, causing a momentary rupture. This tearing let calcium, which is abundant in saliva, move into the cells, triggering internal membranes to move up and patch the hole. In addition, in the seconds that the repair required, growth factors, which promote growth of collagen, new cells and blood vessels, leaked out of injured cells.

Honors

Anders Nattestad, DDS, PhD, Marin, Calif., has been named professor and director of undergraduate oral and maxillofacial surgery at University of the Pacific, Arthur A. Dugoni School of Dentistry.

Anders Nattestad, DDS, PhD

MOU Renewed to Further Improve the Nation's Oral Health

The Department of Health and Human Services and the Academy of General Dentistry recently signed a renewed memorandum of understanding to promote Healthy People 2010, the country's disease prevention and health promotion goals and objectives for the second half of the decade.

Renewed from a 2002 MOU, the partnership aims to improve access to preventive oral health services and eliminate oral health disparities.

"Tooth decay and periodontal disease are two of the most common diseases of modern civilization, and poor oral health and untreated oral diseases can have a significant impact on the quality of life," said Vincent Mayher, DMD, MAGD, and AGD's president, in a press release. "The AGD is excited about partnering with HHS to ensure that Healthy People 2010's oral health objectives are fulfilled."

While not a commitment of funds or an obligation, the renewed MOU is a statement of understanding between the AGD and an agency of the federal government with the ultimate goal of improving the oral health of the nation.

The AGD, in an effort to reach Healthy People 2010's objectives, will educate policy makers by continuing to hold events such as the AGD's first-ever advocacy conference, "A Great Dentists Goes to Washington," this past summer. The AGD also will continue to promote the availability of dental continuing education opportunities at the AGD's annual meeting and constituent venues.

What's in a Name? Plenty, So Be on Guard

While one's identity is unique, theft of it is not.

Last year, more than 246,000 complaints of identity theft were made to the Federal Trade Commission. Most of the time, said Robert LeChevallier in a recent issue of *Membership Matters*, a publication of the Oregon Dental Association, identity theft occurs without the victim aware of it – until the bills arrive.

LeChevallier, an attorney in Lake Oswego, Ore., suggested minor preventive measures such as:

- Never carry your Social Security card or number,
- Limiting the number of credit cards you carry, and
- Shredding all personal information before throwing away papers.

If one does become a victim of identity theft, one should:

- Call the fraud department of the major credit bureaus and ask that a "fraud alert" be placed on your file. This prevents new accounts being opened under your name.
- Call fraud representatives of the companies you believe were targeted. Close those accounts. Follow up with certified mail and include copies of supporting documents.
- File a complaint with the FTC. This can be done online at www.ftc.gov.
- File a report with the police. This paperwork may be needed to prove to banks and credit companies that the fraud occurred.

UPCOMING MEETINGS

2007	
Nov. 27-Dec. 1	American Academy of Oral and Maxillofacial Radiology 58th Annual Session, Chicago, aaomr.org.
2008	
May 1-4	CDA Spring Scientific Session, Anaheim, 800-CDA-SMILE (232-7645), cda.org.
Sept. 12-14	CDA Fall Scientific Session, San Francisco, 800-CDA-SMILE (232-7645), cda.org.
Oct. 16-19	American Dental Association 149th Annual Session, San Antonio, Texas, ada.org.

To have an event included on this list of nonprofit association continuing education meetings, please send the information to Upcoming Meetings, CDA Journal, 1201 K St., 16th Floor, Sacramento, CA 95814 or fax the information to 916-554-5962.

Cadent Introduces the 'Next Generation' iTero Digital Impression System

Cadent recently announced the next generation iTero Digital Impression System is now available for purchase. The new upgrades include faster scanning time, expanded shade libraries, and modified foot pedal design. These enhancements offer users additional flexibility in designing superior fitting prosthetics. The system is commercially available in more than 30 states, and the company anticipates it will be available nationwide by mid-2008. For more information, go to www.cadentitero.com.

Size Doesn't Matter. Or Does It?

In a study of anxiety and needle size, there was no difference in the pain that patients perceived when using larger-diameter needles, authors reported in a recent issue of *General Dentistry*, the Academy of General Dentistry's clinical, peer-reviewed journal.

Michael J. Wahl, DDS, one of the authors, said there was no difference in the pain that patients perceived when using larger-diameter needles. "Many assume that small diameter needles (and therefore smaller puncture wounds) mean less injection pain — but that's not what we found. For perceived injection pain, size doesn't matter."

On the other hand, Gene Antenucci, DDS, FAGD, and an AGD spokesperson, feels patients become fearful when they see a needle. "Often times, when a patient sees a needle coming, the pain perception is heightened."

Antenucci suggested a few things dentists can do to alleviate their patients' qualms. "To ease their fears, it often helps to focus on relaxing by breathing regularly and slowly. Patients can also use hand signals to indicate when they are uncomfortable," he said.

"Dental anxiety is a real condition," Antenucci said. "I encourage my patients to speak to me about their concerns. If I am aware of their fears, I will work with them."

Matt Mullin

To help relieve dental anxiety, patients can:

- Avoid caffeine before a dental appointment;
- Eat high-protein foods, which produce a calming effect, unlike sugary foods;
- Focus on breathing slowly and regularly during the procedure. Being nervous can prompt one to hold one's breath, which then decreases oxygen levels, further increasing feelings of panic; and
- Talk to their dentist about specific fears and concerns.

New All-in-One Self-Etch Bonding System from Heraeus Simplifies Restorative Procedures

Heraeus recently announced the release of the new seventh-generation iBOND Self Etch, an all-in-one bonding agent that etches, primes, bonds, and desensitizes with just one application. The new, improved product replaces the current iBOND, and requires no mixing. It also offers less technique sensitivity with high bond strength and proven marginal efficacy due to easy evaporation, according to results from 15 scientific outcome studies conducted by Heraeus. For more information, contact Heraeus at (800) 431-1785.

Just How Well Do You Know Your Employees?

Even if you have a practice that is doing well, oral health care professionals should think about the damage that can occur from just one bad hire and some experts recommend criminal background checks of all potential employees, according to Joanna Brown in a recent issue of *CDS Review*, the official publication of the Chicago Dental Society.

Brown wrote that not all criminal history should necessarily prevent the dentist from hiring someone. For instance, a night of drunken mayhem in college a decade ago is not quite the same as embezzling from a recent employer.

Professional background screeners can find public information on an applicant for as little as $10 and most searches take only a few days. Still, more thorough searches are a good investment if one is serious about protecting one's practice.

Not only is the practice at risk directly through embezzlement or theft, but patients and other employees could be victimized by a bad hire. Conducting criminal background checks on job applicants could save a dentist a lot of money and heartache later down the road.

Volunteers Sought for Overseas Program

Health Volunteers Overseas is seeking oral and maxillofacial surgeons to volunteer for two-week assignments in Vietnam throughout 2008.

Volunteers will teach surgery, bone grafts and dental implants at the University of Odonto-Stomatology in Hanoi.

HVO is a private nonprofit organization committed to improving health care in developing countries through training and education. Emphasizing teaching rather than service, HVO aims to create an indigenous group of trained health workers who can teach others. This builds an ongoing capability that benefits the population long after the volunteer has departed. Dentists volunteer at sites worldwide, including Cambodia, China, Laos, Nicaragua, Vietnam, and St. Lucia. Assignments vary from one to four weeks.

The Dentistry Overseas division of HVO is sponsored by the ADA and all volunteers must be ADA members.

Housing is provided for volunteers at some program sites, however, they are responsible for all expenses incurred. For more details, go to www.hvousa.org.

Oral Health Services for HIV/AIDS Patients Funded by New Grants

The Health Resources and Services Administration has announced that oral health care is among the services funded by $22 million in new grants for early intervention HIV/AIDS care for medically underserved populations.

Community-based health centers, migrant health centers, hospitals, and other facilities — 53 in all; in 23 states and Puerto Rico — will receive early intervention services grants under the Ryan White HIV/AIDS Program, the agency said. The grants support oral health, nutritional, medical, psychological, and other treatment for patients who are HIV-positive.

A list of grant recipients is available at the HRSA Web site, http://newsroom.hrsa.gov/releases/2007/PartCgrantsJuly2007.htm.

Heraeus Kulzer Introduces Venus Temp C&B

Heraeus Kulzer, Inc., says patients undergoing a temporary restoration can now enjoy the same esthetics found in final restorations with its newest product, Venus Temp C&B. At the same time, dental professionals will appreciate the product's unique combination of strength and beauty. Venus Temp C&B is indicated for the fabrication of esthetic temporary crowns and bridges, inlays, onlays, and veneers. Additionally, its unique and proprietary formulation makes it ideal for long-span bridges. For more information, call (800) 431-1785 or go to www.Heraeus-Venus.com.

MORAYS, CONTINUED FROM 833

UCD. The research shows the amazing diversity possible among living things, even in something as fundamental as feeding, she said in an interview.

Mehta likened the moray eels to snakes, which also have the challenge of trying to ingest a large object using a small opening and fitting it into an elongated and slender body. Snakes have the ability to separate both of their jaws. They are able to seize their prey with one side of their jaw while working the other side around it.

When not in feeding mode, the mobile jaw is just behind the skull of the moray eel. But when propelled forward, the pharyngeal mouth moves nearly the length of the skull. If the outer jaw is able to capture its prey and hold it with a few teeth, the inner set of choppers can secure the food, said Mehta and Wainwright.

Other fish have pharyngeal jaws that function to mince their meal, although "nothing this spectacular," said Wainwright, professor of evolution and ecology at UCD and co-author with Mehta on the research paper that appeared in the Sept. 6 issue of *Nature*.

Using a high-speed digital camera, the sequence of this two-part collaborative feeding system was captured while the eels were feeding in a laboratory. Also used was other imaging equipment and X-ray to determine how the tandem jaws could move. Researchers currently are trying to determine how the pharyngeal mouth developed.

While it has been known that numerous fish species have tucked into their throat extra jaws that pulverize the prey or filter food from the water, the moray eels' newly discovered secret are the first known to assist in entrapping a meal instead of just being part of the gulping process.

Suction is how most fish feed, including the American eel Anguilla. Other fish are adept at snatching their food in their jaws or overtaking their next meal with a wide open mouth. But even then, most fish then rely on suction to move it from their jaws to their esophagus.

Mehta discovered, however, that moray eels have little ability to generate suction through their mouths.

There are more than 200 moray eel species and they can be found all over the globe in tropical waters, making their homes in coral reefs and rock cavities. Some can grow to a length of 10 feet in the wild.

In a newspaper interview, Mark Westneat of the Field Museum of Natural History in Chicago said the discovery is reminiscent of a time when natural phenomena was discovered instead of developing theories and setting out to prove them. He noted it was "a classic example of discovery-based science, stemming from a 'wow' moment."

If the outer jaw is able to capture its prey and hold it with a few teeth, the inner set of choppers can secure the food.

— RITA MEHTA AND PETER WAINWRIGHT

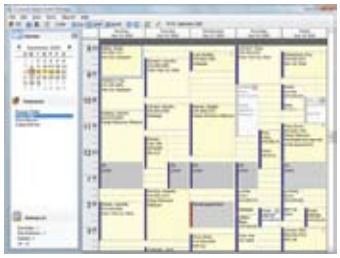

Atlas Business Solutions Introduces Patient Appointment Manager 3.0

Patient Appointment Manager 3.0 is an electronic appointment book designed to keep track of multiple schedules and organizes patient information all in one place. Users can quickly find available appointments and make changes. Features include the ability to customize fields, create service templates with a set duration and color scheme for each service, book repeat appointments, manage waiting lists, send appointment reminders via e-mail or letter, e-mail appointment schedules to employees via a Web browser or PDA, and export or print reports. For more information, call (701) 235-5226 or go to www.abs-usa.com.

Life Insurance Proceeds Can Be Taxed

While death proceeds from a life insurance policy are generally income tax-free, people should be aware they are subject to other forms of taxation, said Dick Cavaliere, in an issue of the *WSDA News*, the journal of the Washington State Dental Association.

The proceeds of a life insurance policy will be included in your estate, and subject to estate taxes, if your estate is named as the beneficiary, or if you have "incidents of ownership" in the policy (e.g., the power to change beneficiaries, borrow against the cash values, etc.), said Cavaliere, director of insurance services, Washington Dentists' Insurance Agency. The proceeds will also be included in your estate if you make a gift of your policy and subsequently die within three years.

And even though federal law permits for an unlimited amount of assets to be transferred to one's spouse without subject to gift or estate taxation, it's key to remember that when the surviving spouse dies, the money is then included in the estate and then is subject to taxation, said Cavaliere. An irrevocable life insurance trust for grandkids or children can remove the proceeds from an estate subject to taxation.

CDA JOURNAL, VOL 35, Nº12

Dental Student RESEARCH

CHARLES GOODACRE, DDS, MSD

GUEST EDITOR

Charles Goodacre, DDS, MSD, is dean of Loma Linda University School of Dentistry.

Dental students become our future practitioners, teachers, researchers, and leaders of organized dentistry. They are the individuals who will produce advances in science, technology, and skills keeping dentistry positioned at the forefront of the health sciences. It is appropriate we regularly recognize the incredible strengths of our students and this issue is focused on such recognition.

The scientific articles in this volume represent the research activities of dental students in our California schools. I continue to be impressed with the escalating level of expertise embodied in today's dental students.

I hope you enjoy reading these articles as they illustrate the bright future for dentistry and dental education in California.

CDA JOURNAL, VOL 35, Nº12

University of California
San Francisco
UCSF
School of Dentistry

DNA Promoter Hypermethylation in Saliva for the Early Diagnosis of Oral Cancer

C.T. VIET; RICHARD C.K. JORDAN, DDS, PHD; AND BRIAN L. SCHMIDT, DDS, MD, PHD

ABSTRACT Oral health care professionals could drastically improve the quality of life for patients with potentially malignant oral lesions by using a noninvasive test that could be used to detect cancer using saliva. Promoter DNA hypermethylation is a critical step in oral carcinogenesis and has a number of significant advantages over genetic and protein diagnostic markers. Methylight is a recently developed assay that rapidly quantifies promoter hypermethylation and could potentially be applied into a clinical setting.

AUTHORS

C.T. Viet is a DDS student at the University of California, San Francisco, School of Dentistry.

Richard C.K. Jordan, DDS, PHD, is a professor with the Department of Orofacial Services, University of California, San Francisco; with the Department of Pathology at UCSF; and with the Comprehensive Cancer Center at UCSF.

Brian L. Schmidt, DDS, MD, PHD, is associate professor at the University of California, San Francisco, Department of Oral and Maxillofacial Surgery, and the UCSF Comprehensive Cancer Center.

DISCLOSURE

Support: NIDCR K12 DE14609

Oral cancer continues to be a significant health problem that affects 40,000 people in the U.S. each year.[1-2] In the U.S. more people die from oral cancer than melanoma, cervical, and ovarian cancer combined.[3] Early diagnosis significantly improves tumor control and survival. The five-year survival for patients with stage I or II oral cancer is 70 percent to 80 percent. In contrast, patients with stage III or IV oral cancer have a survival rate of only 40 percent to 50 percent. Dental health care professionals are commonly required to evaluate patients with potentially malignant oral lesions. There is currently no method to differentiate between patients with oral cancer and oral dysplasia without performing a biopsy. The development of a noninvasive diagnostic method, such as salivary analysis, could be used for oral cancer screening leading to an early diagnosis and an improvement in a patient's quality of life.

For a diagnostic test to be implemented clinically, the test must detect an event in oral cancer patients that is not otherwise present in normal individuals. One such event is methylation of cancer-associated genes, which leads to a loss of function for the gene. Methylation is an epigenetic alteration that involves the addition of methyl groups to cytosine residues in a CpG dinucleotide. It occurs in the promoter region of a gene, where there is a high density of CpG dinucleotides. In fact, promoter hypermethylation is a more frequent mechanism in gene silencing than genetic mutation.[4] It is one of the earliest events in oral carcinogenesis, preceding changes in

protein expression level. These advantages make promoter hypermethylation a very attractive diagnostic marker for the early detection of oral cancer.

The hypothesis of this project is that the presence of oral cancer leads to changes in promoter hypermethylation that could be detected in the saliva of patients. Moreover, salivary analysis based on hypermethylation could be used to noninvasively screen patients at risk for oral cancer.

The first objective of this project, therefore, is to quantitatively analyze promoter hypermethylation of five genes *(APC, E-cadherin, MGMT, p15(INK4B)*, and *p16(INK4A))* in the saliva of three groups of patients: normal, dysplasia, and cancer. Current studies with tissue DNA reveal these genes are most often inactivated by promoter hypermethylation, allowing for the progression of oral cancer.[5-7] **TABLE 1** lists the five genes and their role in carcinogenesis.

Even though quantifying promoter hypermethylation from saliva DNA could be a robust diagnostic tool due to the noninvasive nature of the test and the possibility of detection at the earliest stages, to date, the studies analyzing promoter hypermethylation in saliva DNA have only been qualitative.[8-10] This project is unique because it will be the first to quantitatively measure promoter hypermethylation in saliva DNA, which would allow for higher sensitivity.

Tissue DNA has successfully been used to quantify promoter hypermethylation, but high-quality saliva DNA is much more difficult to isolate than tissue DNA.[11-13] Since this is the first time anyone is quantifying promoter hypermethylation in saliva DNA, it is necessary to establish the validity of using saliva DNA in a quantitative assay. Therefore, the second objective of this project is to determine the correspondence between saliva and tissue promoter hypermethylation. A high positive agreement value between the methylation status of saliva DNA and tissue DNA would indicate saliva is a valid diagnostic medium.

TABLE 1

Role of Genes in Carcinogenesis

Gene	Role in Carcinogenesis
APC	Tumor suppressor
E-cadherin	Synthesizes calcium-dependent adhesion protein involved in metastasis
MGMT	O6-methyl-guanine repair gene
p15	Tumor suppressor; inhibits activity of cyclin-dependent protein kinases, which controls normal progression through G1 of cell cycle
p16	Tumor suppressor; inhibits activity of cyclin-dependent protein kinases, which controls normal progression through G1 of cell cycle

MATERIALS AND METHODS

Promoter Hypermethylation Quantification in Saliva

SALIVA COLLECTION

A faculty mentor routinely sees patients with oral dysplasia and oral cancer. Fourteen patients with either biopsy-proven oral SCC or oral dysplasia at the sites indicated in **FIGURE 1** who have not been previously treated for oral SCC or oral dysplasia, were recruited into the study from the clinical practice of the faculty mentor at the University of California, San Francisco. Saliva was collected before surgical resection. Five normal subjects with no history of oral lesions were also recruited. Whole saliva, 7.5 ml, was collected from oral cancer patients, dysplasia patients, and normal subjects between 6:30 a.m. and 8 a.m. Following collection, saliva samples were stored in a -80-degree Celsius freezer.

DNA Extraction and Modification

Genomic DNA was extracted from 1000 µl saliva with a commercially available DNA extraction kit (QIAamp Blood Kit; Qiagen Hilden, Germany). The DNA was chemically modified with sodium bisulfite to convert all unmethylated cytosines to uracils while leaving methylated cytosines unconverted (EpiTect Bisulfite Kit, Qiagen Hilden) and eluted in 20µl elution buffer. Such modification allowed for differentiation between methylated and unmethylated DNA using Methylight.

Methylight

Methylight, a fluorescence-based real-time PCR assay, was employed to detect methylation in the promoter region of the genes of interest. Three oligonucleotides, a forward primer, reverse primer, and probe were designed for each of the five genes, *APC, E-cadherin, MGMT, p15*, and *p16*. These oligonucleotides annealed within the promoter region of each gene to quantify its methylation status. They were specific to the methylated version of DNA that was unconverted by the sodium bisulfite treatment. The primers, therefore, only amplified methylated DNA and left unmethylated DNA unamplified. The probe was linked to a 5' FAM, 6-carboxyfluorescein, reporter and a 3' Black Hole Quencher (BHQ) dye. During PCR amplification, the reporter dye was separated by the 5'→3' exonuclease activity of DNA polymerase and its fluorescence was measured.

The fluorescence was plotted on an amplification curve; the Ct value obtained from the amplification curve was used to quantify the amount of DNA

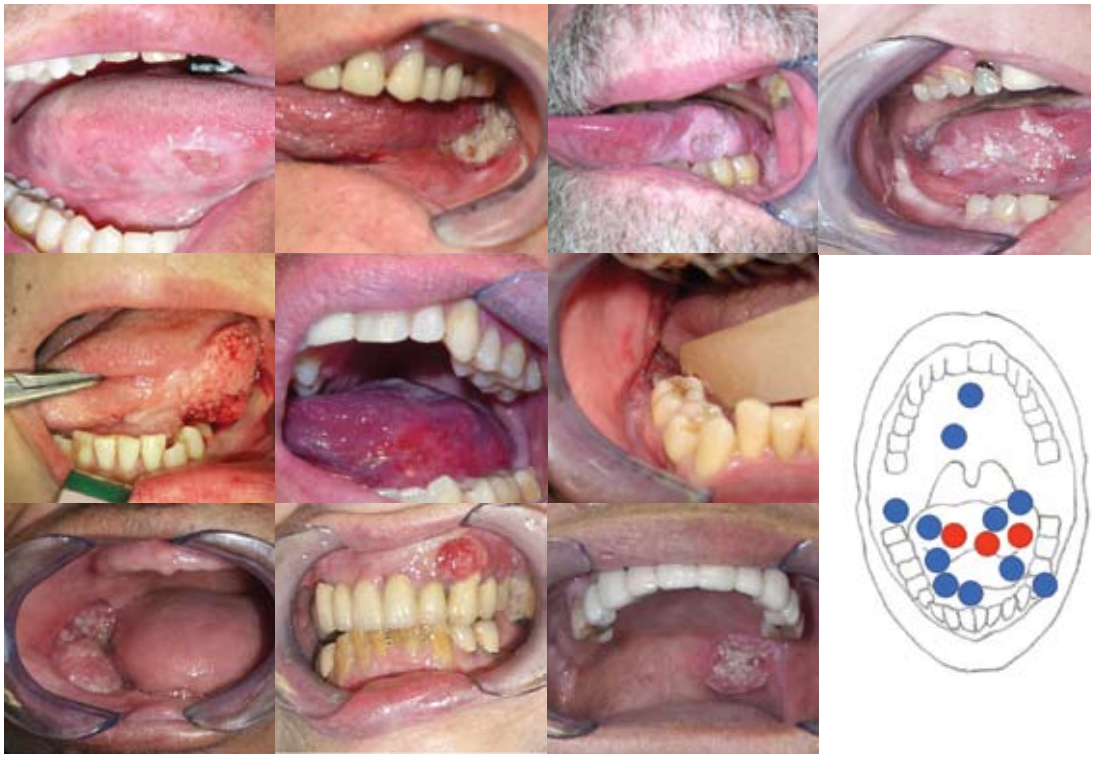

FIGURE 1. The location of oral lesions is indicated with blue representing cancer and red representing dysplasia. Sites include: tongue, floor of mouth, maxillary and mandibular gingiva, and hard and soft palate.

that was amplified. In addition to the five genes of interest, oligonucleotides were also designed for *COL2A1*, an internal reference gene that would be amplified regardless of the methylation status of the DNA. *COL2A1* was used to normalize for differences in genomic template amounts in each reaction.[14]

For each amplification reaction, 2 µl of bisulfite converted DNA was used. PCR was performed in a 30 µl reaction consisting of 0.3 µM of each primer, 0.1 µM of probe, 200 µM each of dATP, dCTP, and dGTP, 400 µM of dUTP, 6.7 mM $MgCl_2$, 1x TaqMan Buffer A, 1x stabilizer, and 2 U of AmpliTaq Gold polymerase at the following conditions: 95-degrees Celsius for 10 min, followed by 50 cycles at 95-degrees Celsius for 15 s and 60-degrees Celsius for 1 min. Male peripheral blood leukocyte DNA (PBL-DNA; Promega) was modified with SssI-CpG methylase enzyme to generate fully methylated human genomic DNA, and was used as a positive control.

Statistical Methods

PCR was performed for each saliva DNA sample with primers and probes from 1) the gene of interest (*APC, E-cadherin, MGMT, p15*, and *p16*) and 2) the reference gene (*COL2A1*). The Ct value of each sample was used to calculate the quantity of DNA that had been amplified during the run. A ratio of the quantity of DNA amplified from the gene of interest (*GENE*) and the quantity amplified from *COL2A1* was obtained. The percentage of methylation value (PMR) was calculated for each sample by dividing the *GENE/COL2A1* ratio of a sample by the *GENE/COL2A1* ratio of the positive control DNA and multiplying by 100.[15]

A PMR value was calculated for all normal, dysplasia, and cancer saliva DNA samples. A PMR cutoff value was calculated, above which samples were considered to be positive for methylation, by taking the median PMR value of normal samples (if > 0) plus one percentage point. If the median PMR value of the normal samples was 0, the PMR cutoff was 1.[16]

COMPARISON OF PROMOTER HYPERMETHYLATION IN TISSUE AND SALIVA DNA

Paraffinized tissue blocks were obtained from patients whose saliva was collected. Ten 10 micron sections were cut from the blocks and genomic DNA was harvested following a protocol for paraffinized tissue (QIAamp Blood Kit). Bisulfite treatment and Methylight were performed at identical conditions to saliva DNA.

Statistical Methods

PMR values were calculated for each tissue DNA sample. A PMR cutoff was determined from the normal tissue DNA using the same calculations as described previously. Cancer or dysplasia samples with a PMR value above the threshold were considered positive for methylation. A positive agreement value between tissue and saliva DNA was calculated for each of the five genes by comparing the methylation status of the tissue and saliva DNA for each sample.

RESULTS

Promoter Hypermethylation Quantification in Saliva

Results from the calculations showed the proportion of samples in the cancer/dysplasia group that were positive for methylation. From **FIGURE 2**, 35 percent of the samples were methylated at *p16*; 29 percent at *MGMT* and *p15*; 14 percent at *APC*; and 7 percent at *E-cadherin*.

Furthermore, the results showed that 71 percent of the oral cancer/dysplasia samples were methylated for one or more genes; 29 percent for two or more genes; 7 percent for three or more genes; and 7 percent for four or more genes (**FIGURE 3**).

COMPARISON OF PROMOTER HYPERMETHYLATION IN TISSUE AND SALIVA DNA

After performing Methylight on saliva and tissue DNA from corresponding patients, the positive agreement value between tissue and saliva DNA at each of the five genes was determined. From **TABLE 2**, the positive agreement of tissue and saliva DNA of *p16*, *E-cadherin*, *p15*, *MGMT* and *APC* were 87.5 percent; 87.5 percent; 62.5 percent; and 62.5 percent; and 12.5 percent, respectively, with a mean value of 62.5 percent.

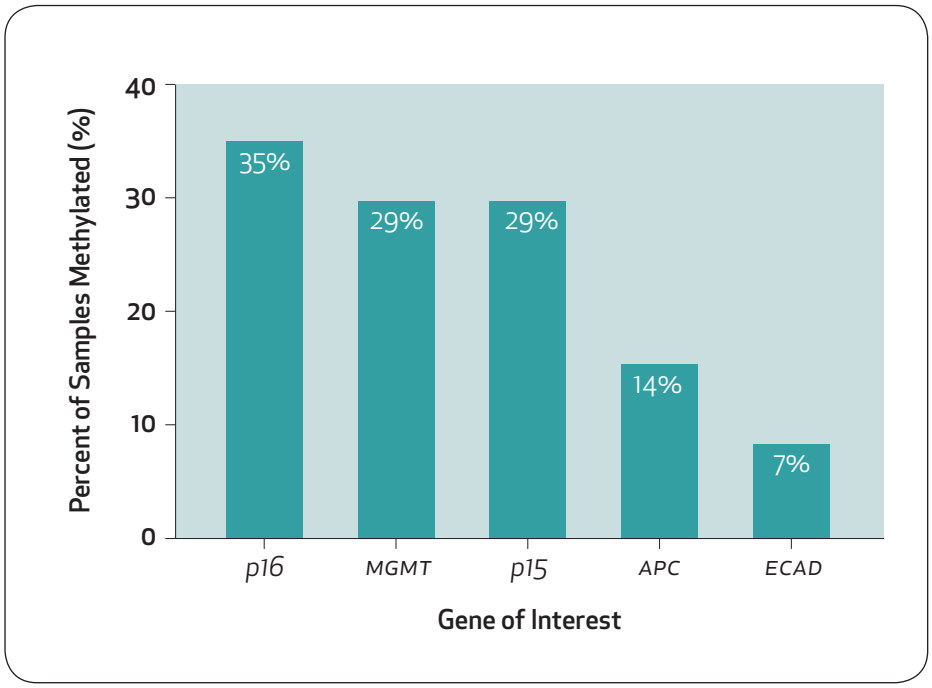

FIGURE 2. The percentage of cancer/dysplasia samples methylated at the corresponding genes is shown.

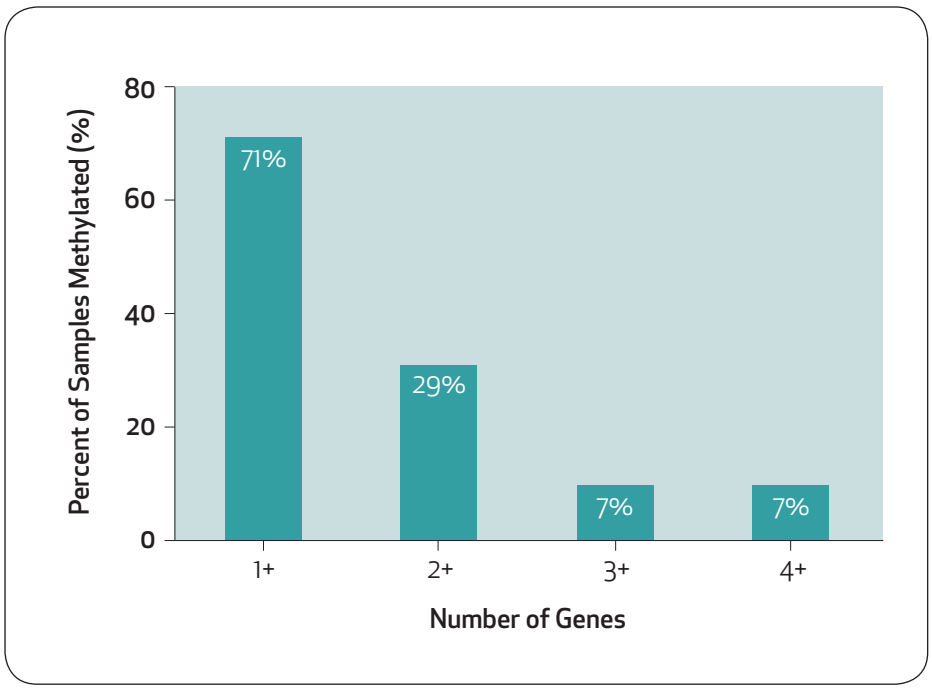

FIGURE 3. Proportion of dysplasia/cancer samples with promoter hypermethylation. The degree of methylation (indicated as PMR value) was measured in dysplasia/cancer (n=14) and normal samples (n=5). PMR values of the normal sample were used to set a normal threshold. Of the dysplasia/cancer samples, 71 percent crossed the threshold and were considered methylated at one or more genes.

CDA JOURNAL, VOL 35, Nº12

DISCUSSION

The assay developed in this project quantified the promoter hypermethylation status of five selected genes in saliva DNA. The methylation frequency ranged from 7 percent to 35 percent for the five genes. Most importantly, using all five genes as a composite biomarker allowed for the detection of 71 percent of the samples.

Furthermore, there was a 62.5 percent agreement between the matched tissue and saliva samples. Saliva has a heterogeneous cell population that makes DNA isolation from cancer cells in saliva more difficult than in tissue. However, the high positive agreement obtained from the assay proved that saliva is a valid diagnostic medium in quantitative methylation-specific PCR techniques.

These results indicate the assay composed of the five selected genes is a promising early marker for cancer detection. Moreover, saliva serves as a potentially ideal medium for future noninvasive diagnostic tests.

The major advantage of using saliva DNA with the Methylight assay is the convenience and noninvasiveness of the assay. Methylight allows for the concurrent analysis of multiple genes in multiple patients in less than two hours. In addition, the assay quantitatively measures the methylation of DNA in cancer and dysplasia samples, providing higher sensitivity than previous qualitative studies that have had to use a gel-electrophoresis-based method to visualize the

ABLE 2

Correlation of Promoter Hypermethylation between Tissue DNA and Saliva DNA

An average correlation of 62.5% was obtained, indicating that saliva DNA is reliable in quantitative methylation-specific PCR techniques.

Gene	Correlation
p16	87.5%
E-cadherin	87.5%
p15	62.5%
MGMT	62.5%
APC	12.5%

amplified DNA and estimate the amount of methylation from the intensity of the DNA bands. Higher sensitivity enables detection of methylation in samples that would have otherwise been overlooked in such qualitative assays.

The convenience, sensitivity, and noninvasive nature of the assay make it a practical method in monitoring disease progression. The assay is currently being evaluated for its capability of predicting dysplasia progression. To date, there is no clinical or molecular method to determine which oral dysplasias progress into cancer.

Furthermore, the assay will be utilized to monitor oral cancer patients after surgical resection. Patients treated for oral SCC have a 26 percent to 47 percent of developing a recurrence within two years of surgical resection and an annual 5 percent chance of developing a second oral primary SCC.[17] Once a second oral cancer develops, the five-year survival drops to 25 percent.[17]

Patients treated for oral cancer are extremely difficult to evaluate for oral cancer recurrence because of their distorted oral and pharyngeal anatomy secondary to scarring following surgery and/or radiation. This salivary assay would improve tumor surveillance in this patient population by identifying a threshold or rate of change in promoter hypermethylation. Early recognition of oral cancer through noninvasive salivary analysis would significantly improve the lives of patients at risk for this disease. ■■■■

REFERENCES

1. Boring CC, Squires TS, Tong T, Cancer statistics. *Calif Cancer J Clin* 41(1):19-36, 1991.
2. Silverman SJ, Epidemiology. D.C. Decker Inc., 1998.
3. Vokes EE, Weichselbaum RR, et al, Head and neck cancer. *N Engl J Med* 328(3):184-94, 1993.
4. Stebbing J, Bower M, et al, Epigenetics: an emerging technology in the diagnosis and treatment of cancer. *Pharmacogenomics* 7(5):747-57, July 2006.
5. Ishida E, Nakamura M, et al, Promoter hypermethylation of p14ARF is a key alteration for progression of oral squamous cell carcinoma. *Oral Oncol* 41(6):614-22, 2005.
6. Uesugi H, Uzawa K, et al, Status of reduced expression and hypermethylation of the APC tumor suppressor gene in human oral squamous cell carcinoma. *Int J Mol Med* 15(4):597-602, 2005.
7. Viswanathan M, Tsuchida N, Shanmugam G, Promoter hypermethylation profile of tumor-associated genes p16, p15, hMLH1, MGMT and E-cadherin in oral squamous cell carcinoma. *Int J Cancer* 105(1):41-6, 2003.
8. Lopez M, Aguirre JM, et al, Gene promoter hypermethylation in oral rinses of leukoplakia patients — a diagnostic and/or prognostic tool? *Eur J Cancer* 39(16):2306-9, 2003.
9. Nakahara Y, Shintani S, Detection of p16 promoter methylation in the serum of oral cancer patients. *Int J Oral Maxillofac Surg* 35(4):362-5, 2006.
10. Rosas SL, Koch W, et al, Promoter hypermethylation patterns of p16, O6-methylguanine-DNA-methyltransferase, and death-associated protein kinase in tumors and saliva of head and neck cancer patients. *Cancer Res* 61(3):939-42, 2001.
11. Eads CA, Danenberg KD, et al, MethyLight: a high-throughput assay to measure DNA methylation. *Nucleic Acids Res* 28(8):E32, 2000.
12. Eads CA, Lord RV, et al, Epigenetic patterns in the progression of esophageal adenocarcinoma. *Cancer Res* 61(8):3410-8, 2001.
13. Goldenberg D, Harden S, et al, Intraoperative molecular margin analysis in head and neck cancer. *Arch Otolaryngol Head Neck Surg* 130(1):39-44, 2004.
14. Ogino S, Kawasaki T, et al, Precision and performance characteristics of bisulfite conversion and real-time PCR (MethyLight) for quantitative DNA methylation analysis. *J Mol Diagn* 8(2):209-17, 2006.
15. Trinh BN, Long TI, Laird PW, DNA methylation analysis by MethyLight technology. *Methods* 25(4):456-62, 2001.
16. Sova P, Feng Q, et al, Discovery of novel methylation biomarkers in cervical carcinoma by global demethylation and microarray analysis. *Cancer Epidemiol Biomarkers Prev* 15(1):114-23, 2006.
17. Loree TR, Strong EW, Significance of positive margins in oral cavity squamous carcinoma. *Am J Surg* 160(4):410-4, 1990.

TO REQUEST A PRINTED COPY OF THIS ARTICLE, PLEASE CONTACT C.T. Viet at chi.viet@ucsf.edu.

CDA JOURNAL, VOL 35, Nº12

LOMA LINDA UNIVERSITY
School of Dentistry

Common Orthodontic Appliances Cause Artifacts That Degrade the Diagnostic Quality of CBCT Images

MATTHEW A. SANDERS, DDS; CHRISTIAN HOYJBERG, DDS; CURTIS B. CHU, DDS; V. LEROY LEGGITT, DDS, MS, PHD; AND JAY S. KIM, PHD

ABSTRACT **OBJECTIVE:** This study evaluates artifacts generated by orthodontic brackets in CBCT images. **METHODS:** Cadaver heads with restoration free dentitions were prepared. CBCT scans with four orthodontic bracket materials utilizing thermoplastic carriers and a control were compared in three phases. **RESULTS:** Stainless steel brackets caused statistically significant ($P<0.0001$) differences from the control in the three phases. **CONCLUSION:** These observations support the hypothesis that metallic and nonmetallic orthodontic brackets interfere with the diagnostic quality of CBCT images.

AUTHORS

Matthew A. Sanders, DDS, is with the GPR Program, Jerry L. Pettis Memorial VA Medical Center, Loma Linda, Calif.

Christian Hoyjberg, DDS, is a resident, Orthodontics and Dentofacial Orthopedics, Loma Linda University School of Dentistry, Loma Linda, Calif.

Curtis B. Chu, DDS, has an oral surgery fellowship, Harlem Hospital, New York, N.Y.

V. Leroy Leggitt, DDS, MS, PHD, is with the Department of Orthodontics and Dentofacial Orthopedics, Loma Linda University School of Dentistry, Loma Linda, Calif.

Jay S. Kim, PHD, is with the Center for Dental Research, Loma Linda University School of Dentistry, Loma Linda, Calif.

ACKNOWLEDGMENTS

The anatomy department at Loma Linda University supplied the cadaver heads. Ormco and GAC donated the orthodontic brackets. Dana Koops and Damon Needleman provided technical support for the NewTom 3G scanning procedures. Joni Stephens, Joe Caruso, and Dean Charles Goodacre provided constructive reviews of early and late versions of this manuscript.

Cone-beam computerized tomography is gaining the widespread interest of dental professionals for 3-D imaging of craniofacial structures. Reasons for this interest seem to be centered on several advantageous factors such as: 1) 2-D and 3-D multiplaner chairside imaging; 2) relatively low-cost scanning; 3) low effective radiation dosages (compared with conventional CT scans); 4) high resolution images (isotropic, sub-millimeter voxels); 5) short scanning times; 6) uniform magnification (almost life-size); and 7) low levels of metallic artifacts compared with conventional fan-beam CT.[1-6] The main drawback of CBCT seems to be low contrast resolution.[1-3]

Because of these factors, 3-D CBCT imaging for implant and orthodontic treatment planning has become common in some dental schools.[2,7-10] At one West Coast dental school, most orthodontic patients receive a T1 (time one, before treatment) CBCT scan to evaluate a multitude of 2-D or 3-D questions such as cephalometric analysis, airway morphology, TMJ morphology, root/bone relationships, bone quality, mandibular nerve pathway, and many other 2-D or 3-D questions. An increasing number of patients receive P (progress, during treatment) and/or T2 (time two, after treatment) CBCT scans to evaluate similar questions.[11-14]

Despite the increasing use of CBCT to clarify 2-D and 3-D clinical questions, it remains unclear if CBCT can be used to reliably detect dental defects such as interproximal caries. Under ideal laboratory conditions (dried mandible, no metal restorations), local CT (fan-beam) was shown to be superior to conventional

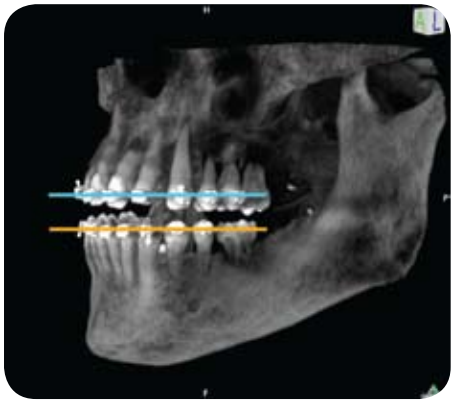

FIGURE 1. A maximum intensity projection of a NewTom 3G scan of a cadaver head showing the maxillary (blue) and mandibular (orange) bracket slot planes. The bracket slot planes are at the same axial level as the interproximal contact planes.

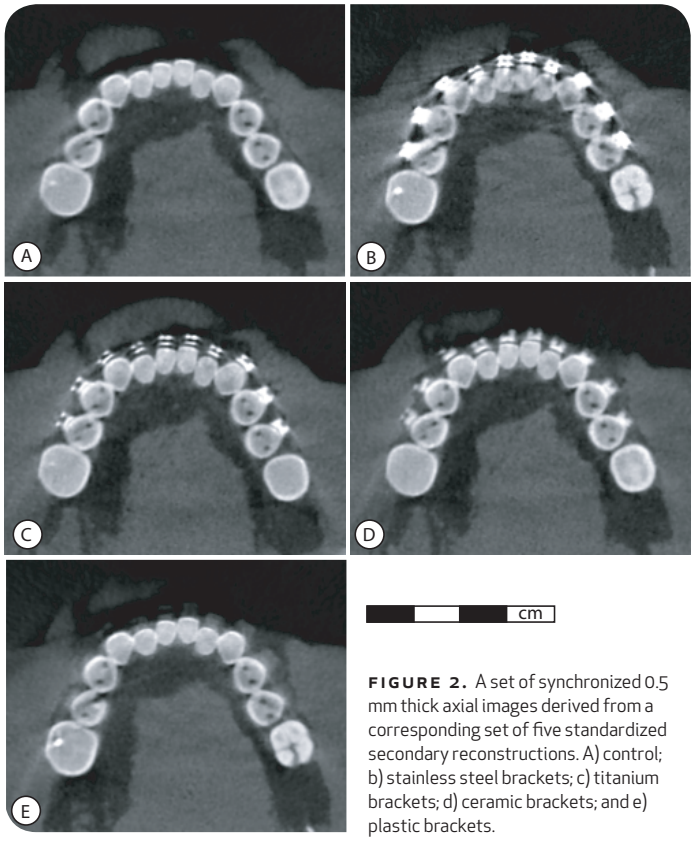

FIGURE 2. A set of synchronized 0.5 mm thick axial images derived from a corresponding set of five standardized secondary reconstructions. A) control; b) stainless steel brackets; c) titanium brackets; d) ceramic brackets; and e) plastic brackets.

bitewing radiographs for interproximal caries detection.[15,16] This improved caries detection using local CT (fan-beam) suggests that other CT systems, such as CBCT, may be helpful in the diagnosis of dental caries. One of the major problems with attempts to use CT (fan- or cone-beam) for evaluation of dental defects is that metallic restorations cause radiographic artifacts in CT images.[1]

Severe streak artifacts, radiopaque and/or radiolucent streaks, around metal restorations or implants are common in fan-beam CT images.[17] In some clinical situations, such as when moni toring a patient for recurrence of head and neck cancer, metallic restorations must be removed and replaced by nonmetallic restorations before fan-beam CT imaging.[17]

Cone-beam CT imaging has been advocated as a radiographic method that strongly reduces metallic streak artifacts.[1] Despite the significant reduction in artifact magnitude, axial CBCT images commonly show light and dark contrast streaks that appear to project radially from metallic restorations. These image streaks cross tooth, bone, and soft tissue structures, and may extend from a metallic restoration completely across the dental arch to contralateral teeth and surrounding anatomic structures.

In addition, less intense streaks can be seen radiating from teeth and other anatomic structures (even in the absence of metallic restorations). It is likely that all radiopaque objects placed in cone-beam CT systems result in some degree of streak artifact that has the potential to affect the image quality of adjacent anatomic structures. These streak artifacts (both obvious and subtle artifacts) have the potential to interfere with accurate interpretation of CBCT images.

The purpose of this paper is to evaluate the effect of common orthodontic appliances on the diagnostic quality axial CBCT (NewTom 3G) images along the bracket slot plane (an axial plane through the occlusal/gingival center of a set of brackets). The authors wanted to evaluate three questions concerning the relationship of orthodontic brackets with CBCT streak artifacts: 1) Can an oral radiologist visually detect streak artifacts caused by orthodontic brackets in axial CBCT

TABLE 1

The Four Bracket Materials Tested

Bracket Material	Trade Name	Company
Ceramic	Inspire Ice	Ormco
Plastic	Vogue	GAC
Stainless steel	MicroArch	GAC
Titanium	Orthos2	Ormco

images?; 2) Do streak artifacts caused by orthodontic brackets change the mean grayscale values of unaltered anterior teeth in axial CBCT images?; and 3) Do streak artifacts caused by orthodontic brackets change the grayscale contrast between artificial dentin defects and the adjacent dentin in axial CBCT images? These questions become increasingly significant to orthodontists as the clinical use of P (progress) CBCT increases.

METHODS

Cadaver and Tooth Preparation

Three cadaver heads were prepared for NewTom 3G scanning by extracting all teeth containing metallic restorations and replacing them with unrestored teeth. The cranial contents had been previously removed from the cadaver heads, however all other tissues were intact. The resultant maxillary and mandibular dental arches contained 12 teeth (first molar to first molar) in each dental arch (**FIGURE 1**). A No. 557 fissure bur was used to drill holes about 1 mm in diameter in the mesial and distal occlusal fossa of all the cadaver premolars (**FIGURE 2**). The holes were drilled perpendicular to the occlusal plane and to a depth below the interproximal contact plane (about 5 mm).

Bracket Placement

Polyvinylsiloxane (Aquasil Monophase: Dentsply Caulk) impressions were made of each dental arch and each impression was poured five times. Orthodontic brackets were aligned on the stone casts with the bracket slots in a single plane of space. This was achieved by tying the bracket slots to a 16 x 22 stainless steel archwire during placement of the brackets on the stone models. The bracket slot plane was aligned with the interproximal contact plane (an imaginary line drawn through the interproximal contacts). An indirect bonding technique was used to attach the brackets on the models using Transbond XT (3M Unitek). Subsequently, the stainless steel archwires were removed.

Thermoplastic trays (Essix) were formed to hold each set of orthodontic brackets (**TABLE 1**: stainless steel, titanium, plastic, ceramic) in ideal positions on the cadaver dental arches (10 brackets per arch). Another thermoplastic tray without brackets was used as a control. Thermoplastic trays with embedded brackets were used to facilitate changing bracket types without normal bonding and removal procedures since these procedures might have caused changes to tooth structure or tooth position.

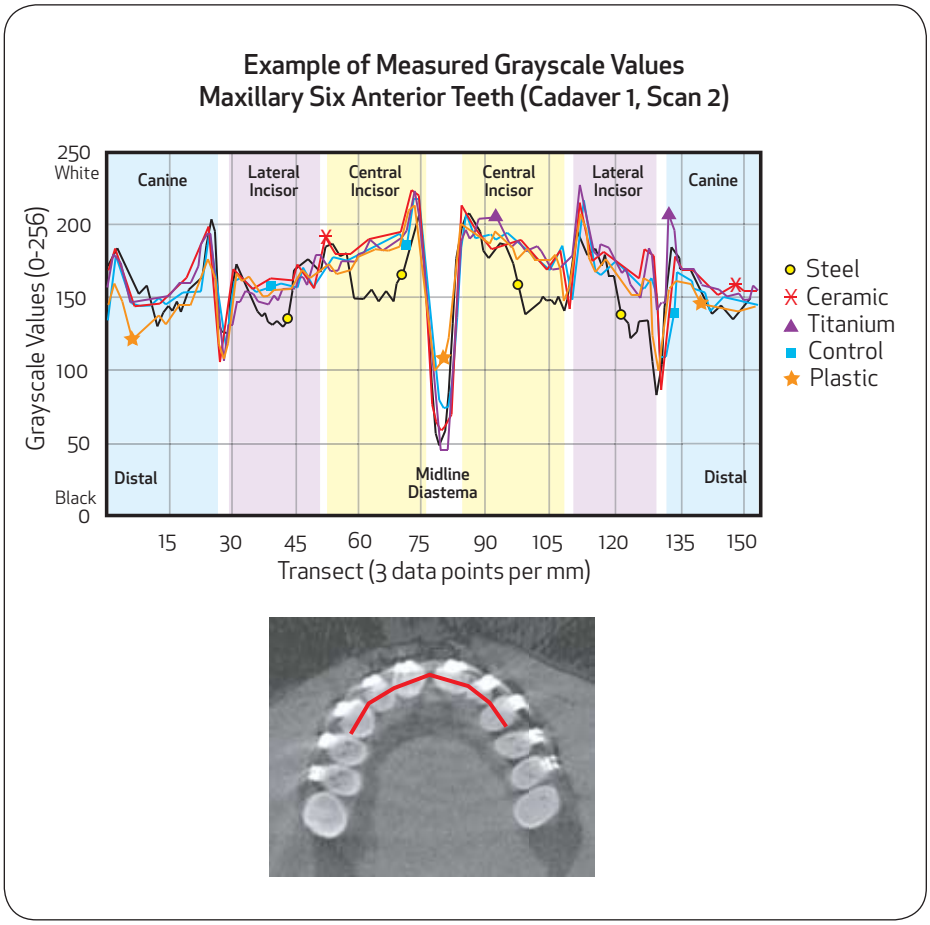

FIGURE 3. An example of measured grayscale values obtained along an interproximal contact transect (red line) of the maxillary six anterior teeth in cadaver No. 1 (scan 2, stainless steel brackets). Dark image areas such as the midline diastema produced low grayscale values. The highest grayscale peaks (lighter) indicate tooth enamel. The central and lateral incisors show depressed grayscale values in the presence of stainless steel brackets. Most data point symbols have been omitted for graph clarity.

Newtom 3g Image Manipulation

Twenty-five, 9-inch volume, NewTom 3G CBCT scans were performed on each cadaver head (five scans per bracket material or control). Primary scanning data was collected in the maxillary and mandibular arches simultaneously. For example, thermoplastic trays containing ceramic brackets were inserted onto both dental arches of a cadaver head, and both arches were scanned in a single 9-inch volume scan. Two

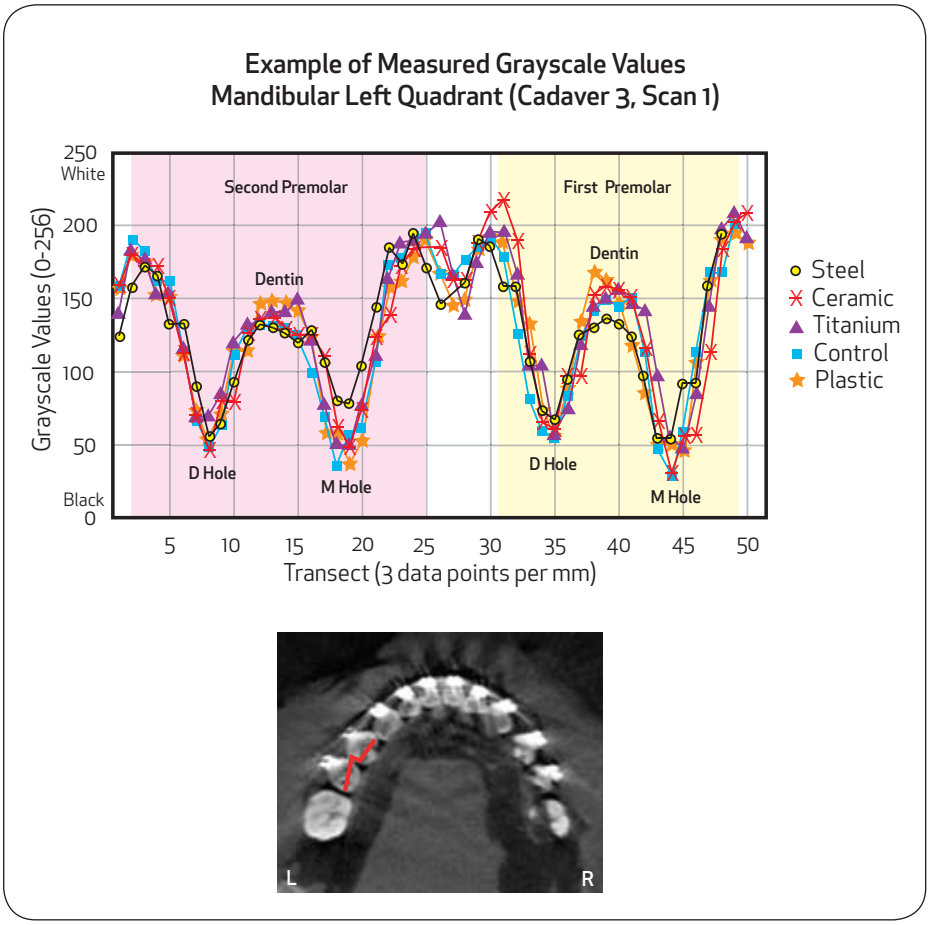

FIGURE 4. An example of measured grayscale values obtained along a transect line (red line) that connects the artificial dentin defects (holes) in the mandibular left quadrant of cadaver No. 3 (scan 1, stainless steel brackets). Low grayscale values are characteristic of the artificial dentin defects. This graph illustrates the decrease in grayscale contrast associated with stainless steel brackets.

secondary reconstructions were done for each NewTom 3G scan (parallel to the maxillary and mandibular bracket slot planes). All 150 secondary reconstructions were performed without image modification (no brightness, contrast, or sharpness changes).

The secondary reconstructions were exported as DICOM files and opened in a common DICOM viewer (OsiriX). Brightness and contrast were optimized for ideal viewing with the naked eye by adjusting a single control scan. All subsequent viewing of secondary reconstructions was done with these control-optimized conditions at life-size. Five secondary reconstructions were viewed simultaneously in OsiriX (**FIGURE 2**). Axial viewing was synchronized and all five scans were simultaneously scrolled equal distances from the incisal edge of the central incisors to the bracket slot plane. This was done to ensure the control scan could be viewed at the same axial level as the bracket containing scans (within 0.5 mm).

When posterior teeth were evaluated, the buccal cusp tips of the first and second premolars were used to synchronize axial plane viewing. Standardized 0.5 mm thick axial slices centered on the bracket slot plane were exported as TIFF image files (**FIGURE 2**).

Analysis of the Resultant Images

The resultant images were analyzed in three ways.

STUDY A — SUBJECTIVE EVALUATION OF ARTIFACTS IN AXIAL IMAGES OF ANTERIOR TEETH

The resultant standardized axial images (**FIGURE 2**) were printed at life-size using a color laser printer and the printed images were evaluated for artifacts by three independent oral radiologists. The radiologists were asked to determine the subjective presence or absence of artifacts (streaks, cross-hatching, or mottling) on each of the six anterior teeth in each scan. If artifacts were present in all six anterior teeth the scan received a maximum score of 6.

The radiologists were asked to use the control images (without brackets) as a baseline; however, they were free to score artifacts in control teeth if they felt artifacts were detectable. The radiologists were not calibrated. Mann-Whitney U-tests were performed at the significance level of α=0.05. Multiple kappa statistics were used to evaluate interrater agreement.

STUDY B — MEAN GRAYSCALE VALUES IN AXIAL IMAGES OF ANTERIOR TEETH

The resultant digital standardized axial images (**FIGURE 2**) were analyzed for objective grayscale differences using a freely available image analysis software program (NIH Image J). A transect line was drawn across the CBCT images of maxillary or mandibular anterior teeth from canine to canine (**FIGURE 3**). The transect line was drawn to intersect the interproximal contact areas of each tooth and grayscale values were sampled at 0.33 mm intervals. An example of grayscale values along a maxillary arch transect line in cadaver No. 1 (scan 2,

CDA JOURNAL, VOL 35, Nº12

TABLE 2

Statistical Significance Using Mann-Whitney U-Tests and Kruskal-Wallis Ranks Tests at the Significance Level of α=0.05.

	Stainless Steel vs. Control	Titanium vs. Control	Ceramic vs. Control	Plastic vs. Control
Study A (Mx)	**P<0.0001**	**P<0.0001**	**P<0.05**	P>0.05
Study A (Md)	**P<0.0001**	**P<0.0001**	P>0.05	P>0.05
Study B (Mx)	**P<0.0001**	P=0.061	P=0.267	P=0.653
Study B (Md)	**P<0.0001**	**P<0.0001**	**P<0.002**	P=0.126
Study C (Mx)	**P<0.0001**	P=0.061	P=0.267	P=0.853
Study C (Md)	**P<0.0001**	P=0.086	P=0.601	P=0.929

stainless steel brackets) is shown in **FIGURE 3**. NIH Image J was asked to return a mean grayscale value for the complete transect for each of the 150 CBCT images. Mean grayscale values for each bracket type were compared with the control using the Kruskal-Wallis ranks test and Mann-Whitney U-test at the significance level of α=0.05.

STUDY C — MEAN GRAYSCALE CONTRAST VALUES BETWEEN DENTIN AND ARTIFICIAL DENTIN DEFECTS

The left half of the mouth was chosen for analysis of grayscale contrast changes between images of artificial dentin defects (drilled holes) and adjacent images of intact dentin. Transect lines were drawn in NIH Image J that connected the mesial and distal holes of each tooth (**FIGURE 4**). An example of grayscale values along a mandibular arch transect in cadaver No. 3 (scan 1, stainless steel brackets) is shown in **FIGURE 4**. Grayscale values were sampled at 0.33 mm intervals. The lightest grayscale value of the dentin between the holes was compared with the darkest grayscale value of each hole. The difference between these two grayscale values was defined as the grayscale contrast between dentin and the artificial dentin defect. Mean grayscale contrast values for each bracket type were compared with the control using the Kruskal-Wallis ranks test and Mann-Whitney U-test at the significance level of α=0.05.

RESULTS

TABLE 2 shows a summary of the results of the statistical tests of the three studies.

Study A

FIGURE 5 shows how the raters scored the axial images of anterior teeth for streak artifacts. Stainless steel and titanium brackets in both arches caused statistically significantly more radiographic artifacts than the control (P<0.0001). Ceramic brackets in the maxillary arch caused statistically significantly more radiographic artifacts than the control (P<0.05). Ceramic brackets in the mandibular arch and all plastic brackets were not statistically different than the control (P>0.05). Multiple kappa statistics showed a low level of agreement on the effect of titanium and ceramic brackets (=0.1369).

Study B

FIGURE 6 shows how the different bracket materials caused variation in mean grayscale values in anterior transects. Stainless steel brackets caused statistically significantly darker mean grayscale values than the control (P<0.0001). In the mandibular arch, titanium (P<0.001) and ceramic brackets (P<0.02) caused statistically significantly darker mean grayscale values than the control. All other mean grayscale values were not different than the control (P>0.05).

Study C

FIGURE 7 shows how the different bracket materials caused variation in mean grayscale contrast between dentin and artificial dentin defects. The stainless steel brackets in both arches caused a statistically significantly difference in mean grayscale contrast than the control (P<0.0001). All other bracket materials produced mean grayscale contrast values that were not different than the control (P>0.05).

DISCUSSION

Orthodontists use progress CBCT scans for a variety of purposes and certainly would like to know if the CBCT images of teeth are altered by inserting orthodontic brackets in the field of view. Since orthodontic brackets are normally aligned in an axial plane of space that is very close to the interproximal contact plane (**FIGURE 1**), any artifacts caused by orthodontic brackets would probably interfere with the diagnosis of dental caries along the interproximal contact plane. This hypothesis is considered likely since CBCT X-ray beams enter the dental arches perpendicular to the long axis of the teeth and pass through orthodontic brackets immediately before they pass through the crowns of the teeth.

This study found significant bracket-induced streak artifacts in axial CBCT images at axial viewing levels that contain the orthodontic brackets. Axial viewing

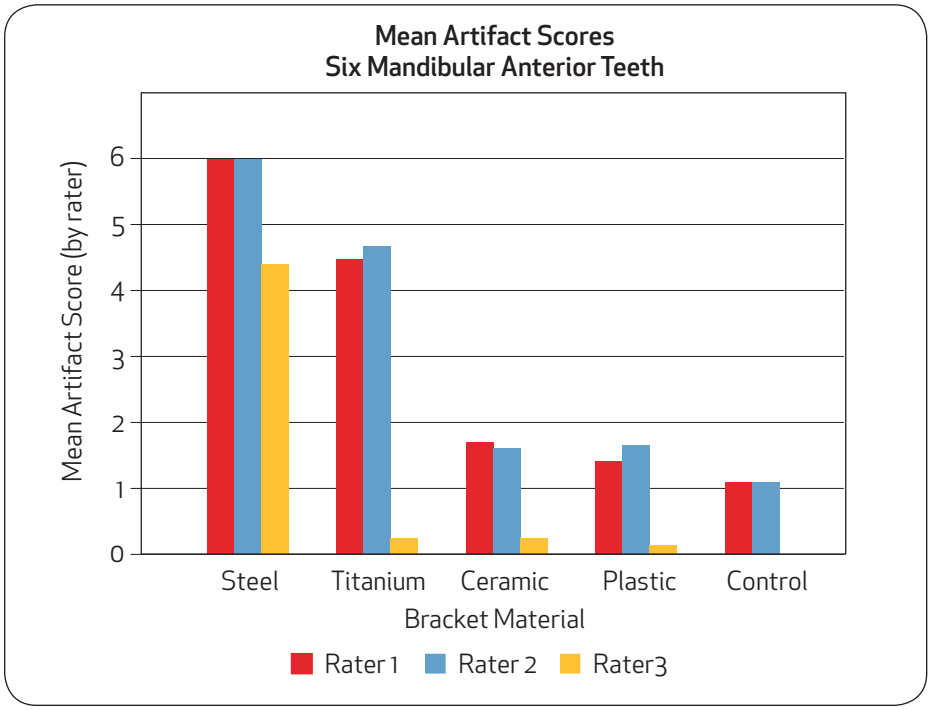

FIGURE 5A.

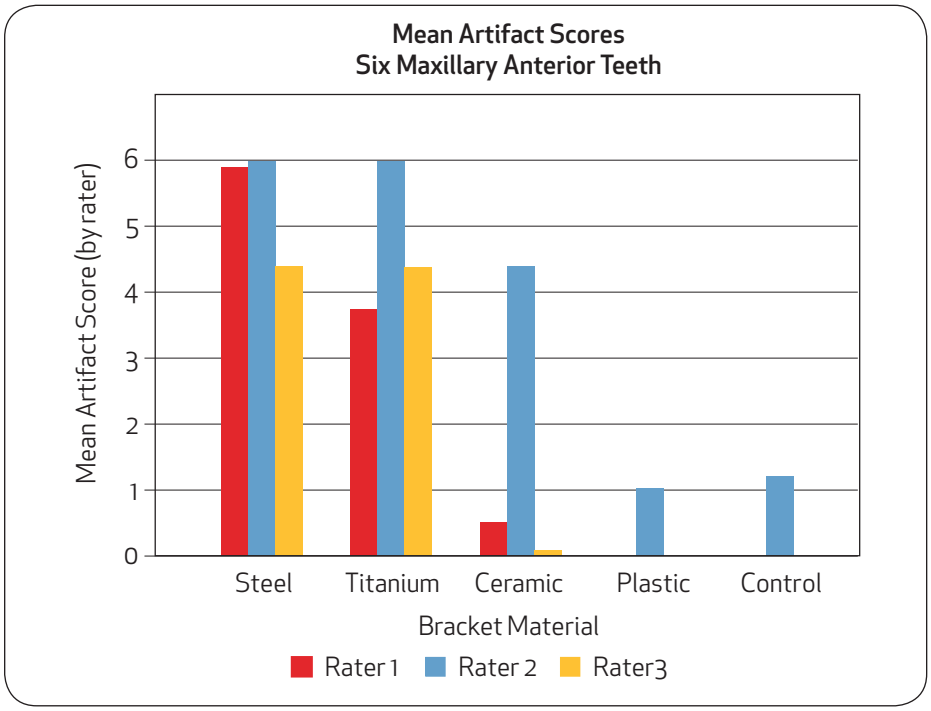

FIGURE 5B.

FIGURE 5. Results of Study A. Mean artifact scores reported by oral radiologists. A) Mandibular anterior mean scores by rater B) maxillary anterior mean scores by rater. No calibration of the radiologists was attempted and this resulted in a low level of agreement between the raters on the effect of titanium and ceramic brackets in the mandibular arch (Figure 5a). In the maxillary arch (Figure 5b); a score of 0 (indicating no detected artifacts) was given by rater 1 and 3 for plastic brackets and for the control. Despite these problems, all raters agreed that the stainless steel brackets caused visually detectable artifacts in both arches.

levels outside the bracket plane zone were not evaluated, however it is not likely that the streak artifacts extend above or below the bracket zone. Since bracket induced streaking should occur roughly parallel to the X-ray beam, artifacts caused by brackets should be confined to axial planes of space that contain the brackets.

Stainless steel brackets were the most significant cause of axial streak artifacts in these CBCT images. These artifacts were detected by changes in the visual appearance of anterior teeth, increases in the radiolucency of anterior teeth and by reduced contrast between dentin and artificial dentin defects in posterior teeth.

In addition to these visual and digital grayscale changes, the grayscale morphology of the streak artifact (horizontal grayscale variation within a single bracket-induced streak) supports the idea that the streaks are caused by orthodontic brackets. **FIGURE 3** shows radiolucent (darker) sawtooth grayscale signatures directly lingual (about 2 mm lingual) to stainless steel brackets (black graph lines with yellow markers). The sawtooth patterns are about the width of an orthodontic bracket, and it is likely that the teeth of the sawtooth pattern represent grayscale variation directly influenced by the thickness of stainless steel in various parts of the bracket. If this is true, then the observed mottling and crosshatched streak artifacts (**FIGURE 2B**) can be explained by the shape of the orthodontic bracket in axial cross section.

Since NewTom 3G bracket plane streak artifacts are clearly generated by stainless steel orthodontic brackets (and often by other bracket materials), it is not appropriate to rely on these axial plane CBCT images to diagnose dental caries. Furthermore the authors speculated that metallic and nonmetallic dental restorations will also cause streak artifacts that may also interfere with caries diagnosis

in the immediate vicinity of the restoration itself (in areas where recurrent decay may occur). While NewTom 3G CBCT scans provide abundant 2-D and 3-D information, the CBCT images (in the presence of orthodontic brackets and likely in the presence of dental restorations) should be supplemented with more traditional radiographic surveys (bitewing radiographs) in order to maintain a high level of diagnostic quality.

CONCLUSIONS

1) Oral radiologists detected streak artifacts (streaks, crosshatching, mottling) in all study conditions including the control images (with no orthodontic brackets). Oral radiologists consistently reported more artifacts associated with stainless steel and titanium brackets than with the control.

2) Stainless steel and titanium brackets caused axial CBCT images of anterior teeth to appear more radiolucent (lower grayscale values). Ceramic brackets in the mandibular arch had a similar effect on CBCT images.

3) Only stainless steel brackets significantly reduced the contrast between normal dentin and artificial dentin defects.

4) Orthodontic brackets have a significant effect on the diagnostic quality of axial images of teeth at or near the interproximal contact plane. Effects of brackets include increases in radiolucent areas and a reduction in radiographic contrast. Since the interproximal contact plane is often the site of dental caries or dental restorations, it is likely that diagnosis of dental caries at the interproximal contact plane is inhibited by the presence of orthodontic brackets, especially stainless steel brackets. Caution must be exercised in this interpretation because this study did not directly study dental caries on CBCT images. ■■■■

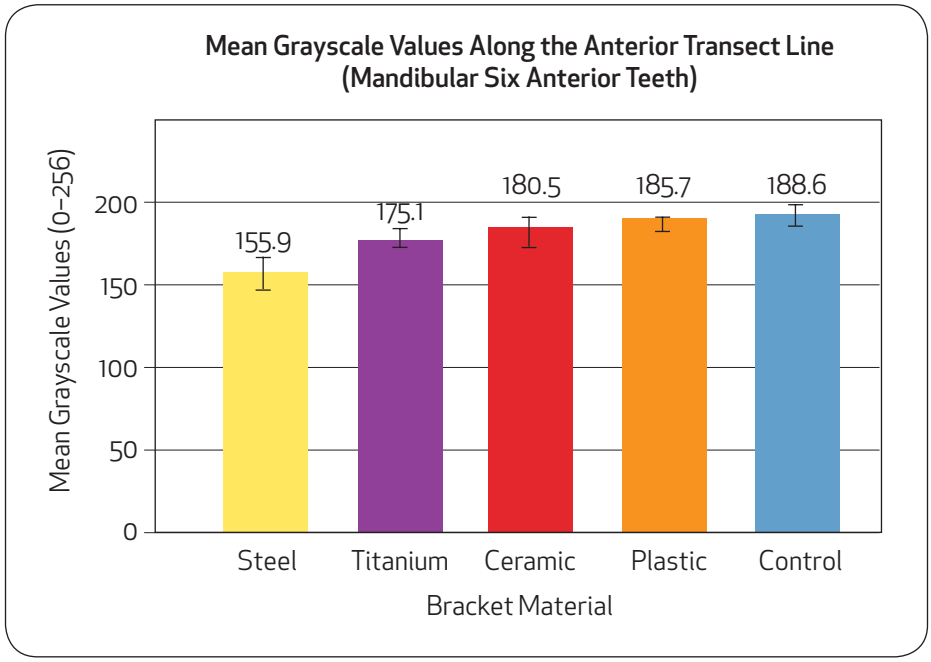

FIGURE 6A.

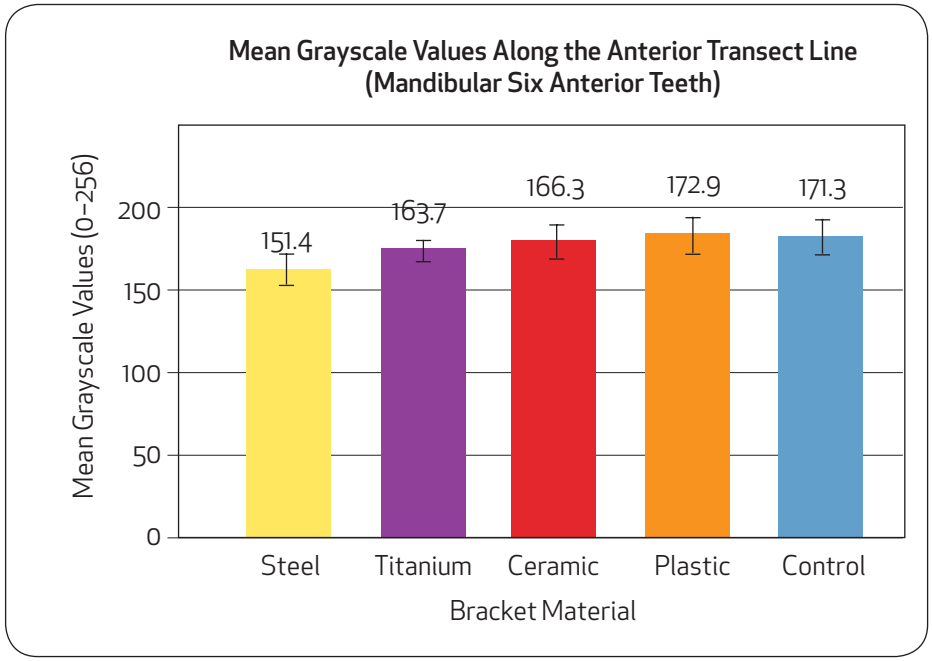

FIGURE 6B.

FIGURE 6. Results of Study B. Mean grayscale values along anterior transect lines. A) Mandibular anterior mean scores; b) maxillary anterior mean scores.

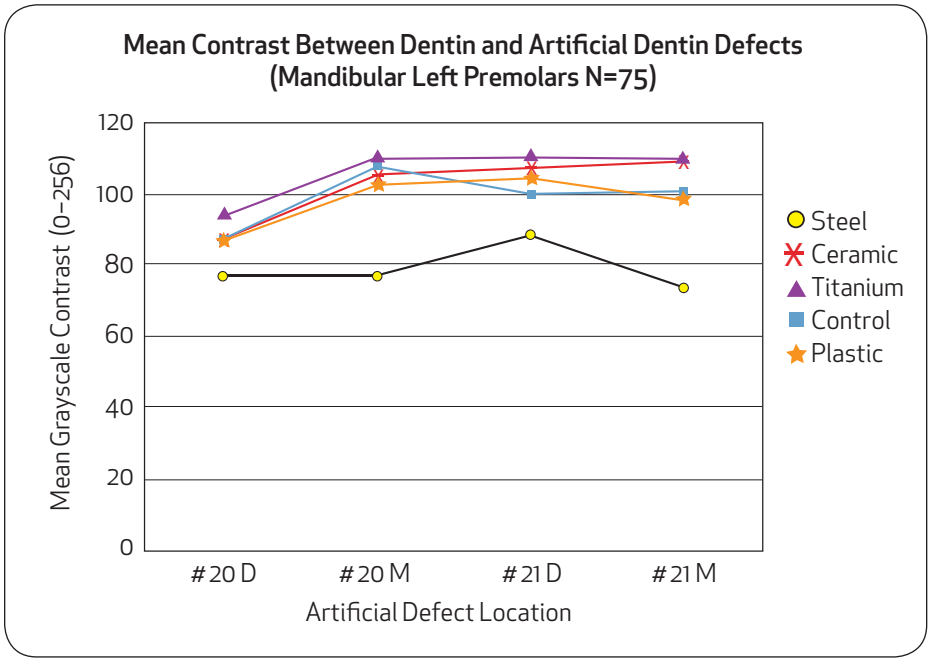

FIGURE 7A.

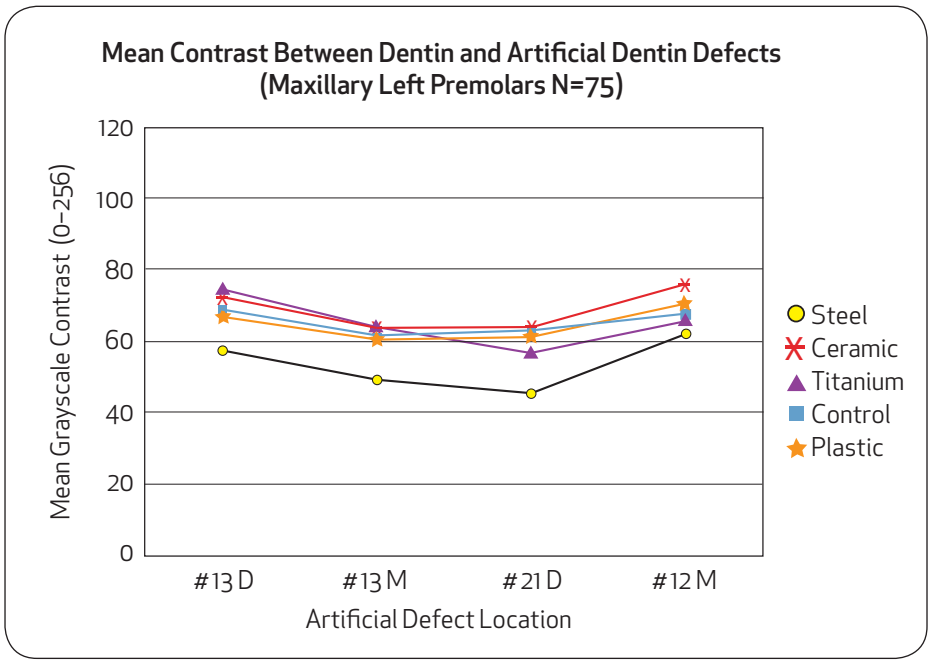

FIGURE 7B.

FIGURE 7. Results of Study C. Mean grayscale contrast values between dentin and artificial dentin defects. A) Mandibular left premolar mean contrast values; b) maxillary left premolar mean contrast values.

REFERENCES

1. Scarfe W, Farman A, Sukovic P, Clinical applications of cone-beam computed tomography in dental practice. *J Can Dent Assoc* 72(1):75-80, February 2006.
2. Kobayashi K, Shimoda S, et al, Accuracy in measurement of distance using limited cone-beam computerized tomography. *Int J Oral and Maxillofacial Implants* 19(2):228-31, March-April 2004.
3. Mozzo P, Procacci C, et al, A new volumetric CT machine for dental imaging based on the cone-beam technique: preliminary results. *Eur Radiol* 8(9):1558-64, 1998.
4. Mah JK, Danforth RA, et al, Radiation absorbed in maxillofacial imaging with a new dental computed tomography device. *Oral Surg Oral Med Oral Pathol Oral Radiol Endod* 96(4):508-13, October 2003.
5. Ludlow JB, Davies-Ludlow LE, Brooks SL, Dosimetry of two extraoral direct digital imaging devices: NewTom cone beam CT and Orthophos Plus DS panoramic unit. *Dentomaxillofac Radiol* 32(4):229-34, July 2003.
6. Marmulla R, Wortche R, et al, Geometric accuracy of the NewTom 9000 cone beam CT. *Dentomaxillofac Radiol* 34(1):28-31, January 2005.
7. Hatcher DC, Dial C, Mayorga C, Cone beam CT for presurgical assessment of implant sites. *J Calif Dent Assoc* 31(11):825-33, November 2003.
8. Hatcher DC, Aboudara CL, Diagnosis goes digital. *Am J Orthod Dentofacial Orthop* 125(4):512-5, April 2004.
9. Mah J, Enciso R, Jorgensen M, Management of impacted cuspids using 3-D volumetric imaging. *J Calif Dent Assoc* 31(11):835-41, November 2003.
10. Erickson M, Caruso JM, Leggitt L, NewTom QR-DVT 9000 imaging used to confirm a clinical diagnosis of iatrogenic mandibular nerve paresthesia. *J Calif Dent Assoc* 31(11):843-5, November 2003.
11. Rungcharassaeng K, Factors affecting buccal bone changes of maxillary posterior teeth after RME. Unpublished Masters Thesis, Loma Linda University 1-32, 2006.
12. Robinson J, Measured effects of rapid palatal expansion on nasal cavity volume utilizing CBCT. Unpublished Masters Thesis, Loma Linda University 1-42, 2003.
13. Hutchinson S, CBCT panoramic images vs. traditional panoramic radiographs. Unpublished Masters Thesis, Loma Linda University 1-45, 2004.
14. Nguyen D, Variability in selecting lateral cephalometric landmarks in two CBCT image modes. Unpublished Masters Thesis, Loma Linda University 1-55, 2006.
15. van Daatselaar AN, Tyndall DA, van der Stelt PF, Caries detection with local CT. *Dentomaxillofac Radiol* 32(4):235-41, July 2003.
16. van Daatselaar AN, Tyndall DA, et al, Minimum number of basis projections for caries detection with local CT. *Dentomaxillofac Radiol* 33(6):355-60, November 2004.
17. Odlum O, A method of eliminating streak artifacts from metallic dental restorations in CTs of head and neck cancer patients. *Spec Care Dentistry* 21(2):72-4, March-April 2001.

TO REQUEST A PRINTED COPY OF THIS ARTICLE, PLEASE CONTACT Matthew A. Sanders, DDS, at msandersdds@yahoo.com.

CDA JOURNAL, VOL 35, Nº12

Microarray Analysis of Bmi-1 Downstream Genes in Normal Human Oral Keratinocytes

FELIX K. YIP; MO K. KANG, PHD, DDS, MS; AND NO-HEE PARK, PHD, DMD

ABSTRACT Bmi-1 is a polycomb group oncogene highly overexpressed in premalignant and malignant oral lesions. Bmi-1 is believed to promote oral carcinogenesis in part by allowing normal cells to evade the senescence checkpoint and extending their replicative life span. To determine the mechanisms underlying the role of Bmi-1 in oral carcinogenesis, the authors performed microarray analysis in normal human oral keratinocytes, NHOK, overexpressing Bmi-1. The authors report here several potential target genes of Bmi-1.

AUTHORS

Felix K. Yip is a dental student at the University of California, Los Angeles, School of Dentistry.

Mo K. Kang, PHD, DDS, MS, is an associate professor, endodontics, Associated Clinical Specialties, University of California, Los Angeles, School of Dentistry, and with the UCLA Jonsson Comprehensive Cancer Center in Los Angeles.

No-Hee Park, PHD, DMD, is dean of the University of California, Los Angeles, School of Dentistry; professor of Diagnostic and Surgical Services at UCLA; with the UCLA Jonsson Comprehensive Cancer Center in Los Angeles and with the David Geffen School of Medicine at UCLA.

ACKNOWLEDGMENTS

The authors thank Dr. Dimri for the Bmi-1 retroviral constructs. This study was supported in part by the grants (DE14147, DE15316, and DE18295) from the NIDCR/NIH and the Oral and Maxillofacial Surgery Foundation.

The senescence process, or "cellular aging," in normal human oral keratinocytes has been studied extensively in the context of its tumor suppressive function. It has been found that the senescence block in NHOK can be overcome by expression of Bmi-1.[1] Bmi-1 is a polycomb group transcription repressor originally found by provirus (Moloney murine leukemia virus; MuLV) tagging to identify the cellular gene cooperating with c-myc in pre-B cell lymphomagenesis.[2] Transgenic mice overexpressing c-myc in their lymphoid tissues develop pre-B cell lymphomas with greater efficiency when infected with MuLV, which was frequently (49 percent) found integrated near the cellular Bmi-1 locus, resulting in increased level of Bmi-1 expression.[2] These findings indicate that Bmi-1 overexpression contributes to tumorigenesis. Recent studies also showed that proliferative capacity of leukemic and normal hemopoietic stem cells derived from Bmi-1-/- mice was compromised, suggesting the possible role of Bmi-1 in the maintenance of tumor stem cell phenotype.[3]

Bmi-1 is believed to promote cellular proliferation by inhibiting the expression of $p16I^{NK4A}$ tumor suppressor protein.[4] During normal replication of human diploid fibroblasts (HDF), Bmi-1 expression level is decreased notably during senescence.[5] When overexpressed, Bmi-1 is able to extend the replicative life span of HDF, HMEC, and NHOK.[5,6,1] Thus, in normal human cells, diminution of Bmi-1 expression may be necessary for the onset of senescence, which can be overcome during carcinogenesis by sustained overexpression of Bmi-1. The association between Bmi-1 and oral carcinogenesis has been studied by Kang et al. who showed that overexpression of Bmi-1 occurs very early in oral carcinogenesis upon dysplatic epithelial transformation and is required

for sustained cancer cell replication and survival.[7] It is possible that Bmi-1 evades the senescence block and results in cellular transformation during oral carcinogenesis.

Identification of the downstream genes of Bmi-1 in oral carcinogenesis is important for understanding the pathophysiology of the disease progression and to identify novel early markers of oral squamous cell carcinoma. With this purpose, the authors expressed exogenous Bmi-1 in rapidly proliferating NHOK and determined its effect on altered gene expression profiles by DNA microarray analysis. The authors found several candidate target gene groups of Bmi-1 in NHOK, including those involved in apoptosis, cell cycle regulation, and DNA replication. Further study is necessary to elucidate their biological roles in oral carcinogenesis.

MATERIALS AND METHODS

Cells and Cell Culture

Primary NHOK cultures were prepared from separated epithelial tissue discarded from routine oral surgery procedures and subsequently serially subcultured in keratinocyte growth medium (KGM) containing a low level (0.15 mM) of Ca^{++} and supplementary growth factor bullet kit (Cambrex, East Rutherford, N.J.) as described previously.[8] Briefly, epithelial cells were isolated from the basal surface of the epithelial tissue of approximately 25 mm^2 × 0.5 mm in size by trypsin digestion. The duration of the enzymatic digestion was limited to three min. to avoid harvesting cells from the suprabasal layers. These cells were seeded onto two collagen-treated T25 culture flasks and allowed to proliferate until 60 percent to 70 percent confluency. Primary NHOK were serially subcultured in KGM, with passage at every 60 percent to 70 percent confluency level.

Retrovirus Construction

For this study, the authors constructed a two retroviral vectors: RV-Bo and RV-Bmi-1. These viral vectors were prepared, respectively, from pBabe and pBabe-Bmi-1 retroviral expression plasmids, which were a kind gift of Dr. Goberdhan Dimri (Northwestern University, Evanston, Ill.). pBabe-Bo or pBabe-Bmi-1 was introduced into GP2-293 packaging cells (BD Biosciences, Bedford, Mass.) by the calcium phosphate precipitation method. Briefly, the day before transfection, GP2-293 cells were plated into T-175 flasks (Corning, Corning, N.Y.) at 1.5 x 10^7 cells, with 30 ml of DMEM (Invitrogen) supplemeted with 10 percent *SCS* (Gemini). Upon 60 percent to 70 percent confluency the next day, media was replaced with 25 ml of fresh media and cells were additionally incubated with 2 ml of 1x Hepes Buffered Saline solution containing 15 µg of pBabe-Bo or pBabe-Bmi-1, 15 µg of pCMV-VSV-G envelope plasmid, and 0.1 mM CaCl. Viral supernatant was collected 24 and 48 hours after transfections, filtered through 0.45 µm-pore-size filter, and harvested at 5 x 10^5 g for 1.5 hrs at 4 degrees Celsius. The resulting viral pellet was then resuspended in 2 ml of KGM overnight at 4 degrees Celsius, aliquoted, and stored at -80 degrees Celsius.

DURING NORMAL replication of human diploid fibroblasts (HDF), Bmi-1 expression level is decreased notably during senescence.

Retrovirus Infection and Selection

NHOK were cultured to ~70 percent confluency in BD Falcon 6-well dishes (BD Biosciences), and subsequently incubated for four hours at 37 degrees Celsius with the retroviral vectors and polybrene (Sigma) at a concentration of 8 µg/ml. The supernatant was then changed with fresh media and the infected cells were selected with puromycin (Sigma) two days after infection at a concentration of 1 µg/ml. The infected cells were then serially subcultured in the presence of puromycin (1 µg/ml) and collected at various time points for further analysis.

RNA Isolation and Analysis of Gene Expression by Microarray

Gene expression profiling was performed between senescing NHOK infected with the empty vector control (RV-Bo) and NHOK with the virus expressing Bmi-1 (RV-Bmi-1), using the GeneChip Human Genome U133 Plus 2.0 Array from Affymetrix (Santa Clara, Calif.).

Total RNA was extracted from cultured NHOK (RV-Bo at population doubling (PD) 12 and RV-Bmi-1 at PD 19) using Trizol reagent (Invitrogen) and further purified through RNeasy columns (Qiagen, Chatsworth, Calif.) using the standard protocol.[9] The probe synthesis, labeling, hybridization, and data acquisition were performed by the DNA Microarray Core facility at University of California, Los Angeles.

The expression profiling of more than 47,000 annotated genes was compared between senescing NHOK 05-12 infected with RV-Bo, and NHOK 05-12 with extended life span infected with RV-Bmi-1. Data analysis was followed after calibrating the Cy3 signals from the two NHOK cultures based on the mean value of the overall signal intensity and the distribution of the individual spot intensities.

CDA JOURNAL, VOL 35, Nº12

RESULTS

Cellular Proliferation and Kinetics of Replication

Primary NHOK undergo a finite number of replications during serial subcultures before entering a senescing phase, characterized by the loss of replicating potential and lack of DNA synthesis, immediately followed by senescence and differentiation. The maximum replication potential of NHOK in the authors' previous report was determined to be 22 ± 3 population doublings (PD).[8] In this study, the NHOK strain used (05-12) reached a maximum accumulated 19 PDs at senescence.

In order to determine the effects of ectopically expressed Bmi-1 on the replicative capacity of NHOK, the authors infected secondary NHOK with RV-Bo or RV-Bmi-1, which represent empty vector and the retroviral vector expressing full-length Bmi-1, respectively. These viral vectors were prepared by transfection of pBabe and pBabe-Bmi-1 plasmids into GP2-293 packaging cells along with pCMV-VSV-G. Transfecting with VSV-G allows for the produced viral particles to be concentrated by ultracentrifugation at 50,000g; this is not otherwise possible because other envelope proteins are linked by weak disulfide bonds that may not withstand centrifugation and filtration.[10]

NHOK were infected with concentrated RV-Bo or RV-Bmi-1 for four hours in media containing 8 µg/µl of polybrene. Polybrene is a small, charged molecule that enhances the efficiency of infection by neutralizing surface charges, facilitating the interaction between the retrovirus and cellular membrane surface.[11] At 24 hours postinfection, 1 µg/µl of puromycin was introduced to the culture medium as a selection marker. The drug-resistant cells were maintained at 70 percent confluence to avoid contact-regulated growth inhibition and differentiation. NHOK stably expressing Bmi-1 were able to extend their replicative potential from a maximum cumulated 19 PDs in RV-Bo infected cells to over 27 PDs in RV-Bmi-1 transduced cells (FIGURE 1), but underwent a delayed senescence and were unable to reach immortalization.

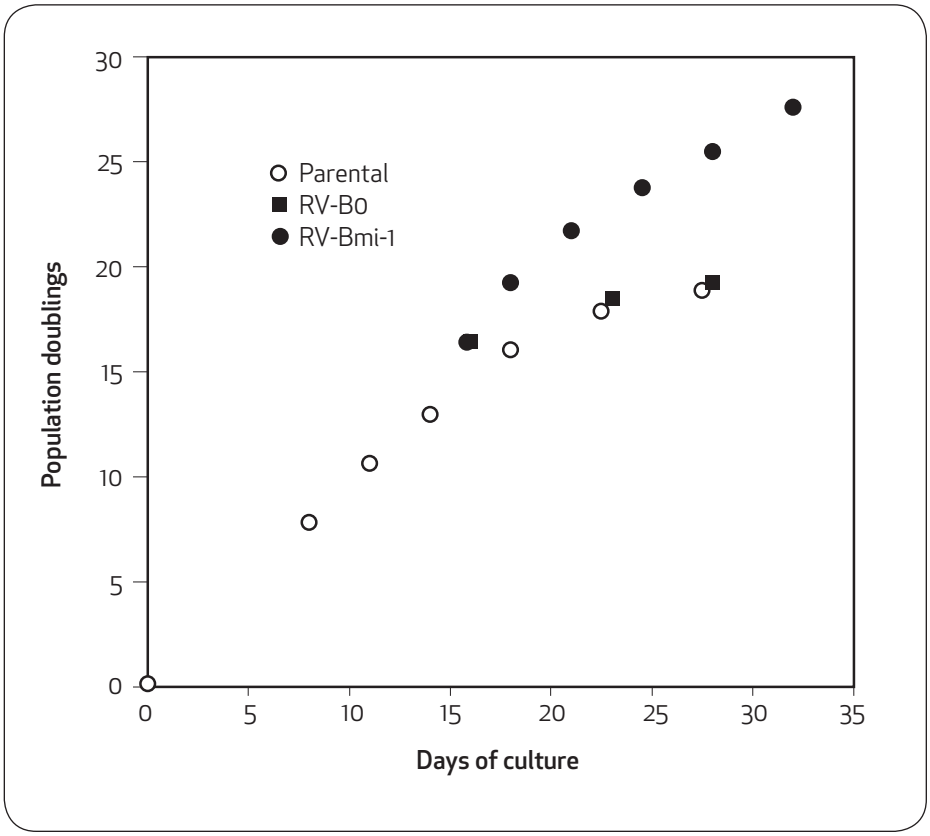

FIGURE 1. Replication kinetics of parental NHOK and NHOK ectopically expressing Bmi-1. Replication kinetics of parental NHOK (Parental); NHOK infected with RV-Bo (RV-Bo); and NHOK infected with RV-Bmi-1 (RV-Bmi-1). NHOK was infected with RV-Bo and RV-Bmi-1 14 days after the initial primary culture of NHOK. Parental NHOK reached a maximum 19 PDs, NHOK/RV-Bo reached a maximum 19 PDs, and NHOK/RV-Bmi-1 reached a maximum 28 PDs.

Differential Gene Expression Profiling in NHOK With or Without Bmi-1 Overexpression

In order to elucidate the potential downstream targets of Bmi-1, RNA was extracted from NHOK infected with RV-Bo and undergoing senescence and NHOK overexpressing Bmi-1 exhibiting an extension of life span (FIGURE 2). Fluorescent-labeled cDNA was prepared from the RNA of senescent NHOK, infected with RV-Bo (NHOK/RV-Bo) at PD 19, and from NHOK overexpressing Bmi-1 (NHOK/RV-Bmi-1) with an extended life span at PD 22. Senescent NHOK/RV-Bo (PD 19) showed characteristics of senescence as previously described, including flattened morphology, perinuclear vacuolization, increased cytoplasmic to nuclear ratio, and SA-β-Gal expression, in contrast to NHOK/RV-Bmi-1 (PD 22), which demonstrated normal morphology and remained in the exponentially replicating phase.[8]

Hybridizing the labeled cDNA to the Affymetrix Human Genome U133 Plus 2.0 Array, the authors were able to analyze the expression of over 47,000 different transcripts corresponding to 38,500 genes. Spot intensities from the microarray were analyzed using Affymetric Gene

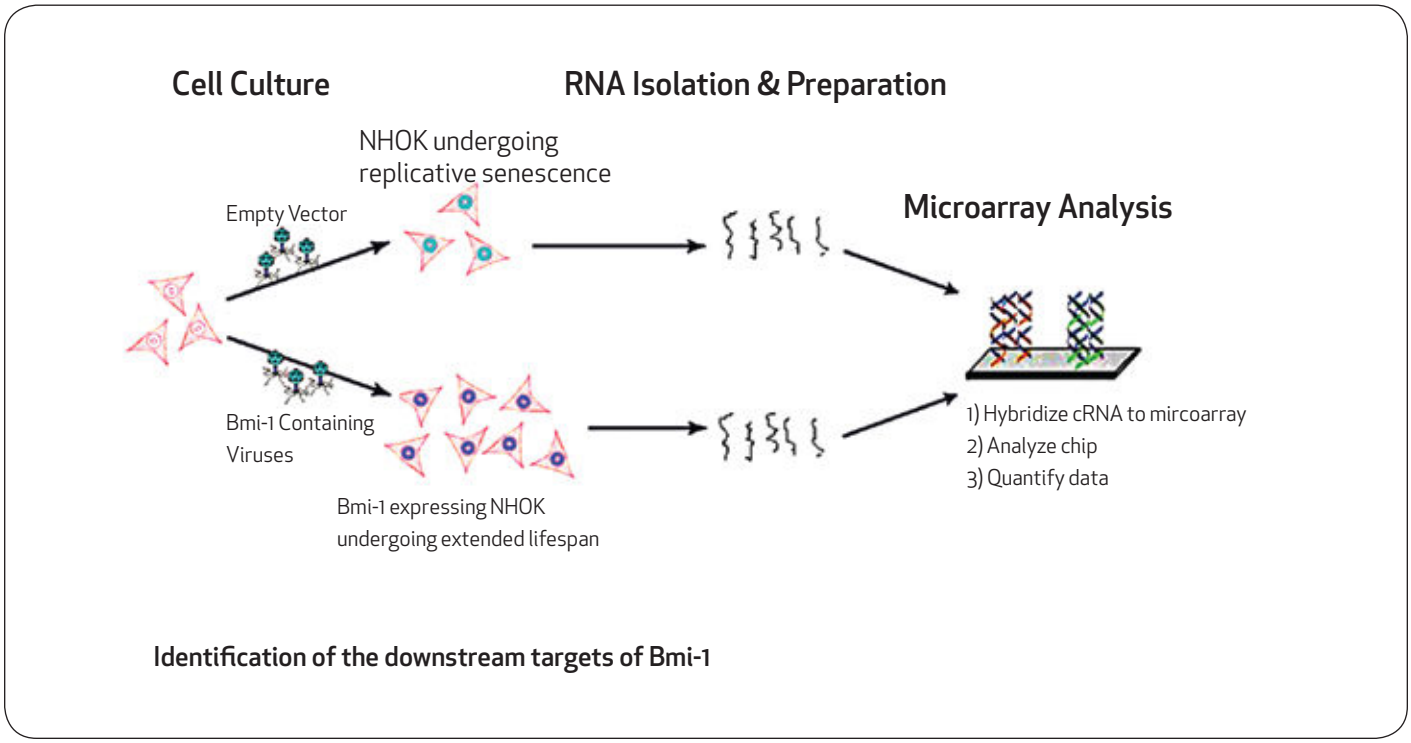

FIGURE 2. NHOK cultured from discarded epithelial tissue was infected with vectors containing Bmi-1. RNA was isolated from NHOK undergoing replicative senescence and Bmi-1 overexpressing NHOK with an extended life span. RNA was hybridized to an affymetrix microarray chip containing probes representing more than 38,000 genes. Chips were analyzed and quantified for intensity of hybridization, and genes with a greater than two-fold difference of expression between the two groups were selected for further study.

Chip Operating Software. Statistically significant ($P<0.05$) differences were further reduced using the selection criteria cutoff (>2-fold difference). As a result, the authors observed a total of 3,024 transcripts that were differentially expressed between NHOK/RV-Bo (PD 19) and NHOK-Bmi-1-(PD 27). Of these, 1,321 genes were upregulated in Bmi-1 overexpressing NHOK, and 1,703 genes were downregulated compared to NHOK/RV-Bo (PD 19). A detailed analysis of their functions was conducted and the genes were grouped into major biochemical pathways, i.e., cell cycle control, cellular differentiation, and apoptosis.

In order to compile a broader understanding of the patterns associated with Bmi-1 expression in NHOK, previous gene expression data were normalized using the Robust Multichip Average. The authors used the RMA Express software developed by the Ben Bolstad group at University of California, Berkeley, in 2003 in order to attain a global perspective on differential gene expression. The protocol consists of three steps: a background adjustment, quantile normalization, and summarization, which ultimately allows for the comparison of data across several experiments. RMA normalization was utilized to allow the comparison of differential gene expression data between genes differentially expressed 1) when Bmi-1 is overexpressed in late passage NHOK (denoted by NHOK/RV-Bmi-1 at PD 19); 2) when Bmi-1 is overexpressed in early passage NHOK (NHOK/RV-Bo at PD 11) and NHOK-RV-Bmi-1 at PD 11); and 3) in parental exponentially replicating and senescing NHOK (NHOK at PD 11) and NHOK at PD 19).

The normalized data were compared using NHOK-RV/RV-Bo (PD 19) as the baseline, in order to demonstrate whether NHOK/RV-Bmi-1 (PD 22) exhibited a pattern of expression more similar to exponentially replicating parental NHOK (PD 11), exponentially replicating NHOK/RV-Bo (PD 11), and exponentially replicating NHOK/RV-Bmi-1 (PD 11), or senescing parental NHOK (PD 19).

Genes were then categorized according to the Affymetrix Netaffx online module Gene Ontology Biological Process and Gene Ontology Molecular Function criteria for further analysis. The TIGR Multiexperiment Viewer software was then used to visualize global gene expression patterns and cluster genes using K-means hierarchical clustering statistical algorithms.

FIGURE 3A shows the global pattern of expression of all 3,024 transcripts that were differentially expressed between NHOK/RV-Bo (PD 19) and NHOK/RV-Bmi-1 (PD 22) in the original microarray data, as compared across all experimental

conditions in a dendrogram heatmap. These genes showed a clear, consistent pattern of expression in NHOK/RV-Bmi-1 (PD 22) with NHOK/RV-Bmi-1 (PD 11), NHOK/RV-Bo (PD 11), and NHOK (PD 11). This is in contrast with NHOK (PD 19), which showed a generally opposite pattern of expression. **FIGURE 3B** also shows the pattern of expression of various apoptosis-related genes, again detailing the opposing pattern of expression in senescing NHOK, but the recovery of exponentially replicating expression via the ectopic overexpression of Bmi-1 in NHOK with an extended life span.

As expected, several genes associated with cell cycle arrest also exhibited a consistent pattern between Bmi-1 overexpressing strains and parental NHOK (PD 11), and an opposing pattern in senescent parental NHOK (PD 19) (**FIGURE 3C**). Lastly, Bmi-1 appears to recover the exponentially replicating pattern of expression of several genes associated with differentiation. Again, the pattern is clear that Bmi-1 overexpressed in extended-life span NHOK allows genes that are otherwise oppositely expressed in senescing NHOK (NHOK (PD 19)) to follow the patterning of exponentially replicating parental (NHOK at PD 11) and Bmi-1 overexpressing NHOK (NHOK/RV-Bo at PD 11, NHOK/RV-Bmi-1 at PD 11) (**FIGURE 3D**).

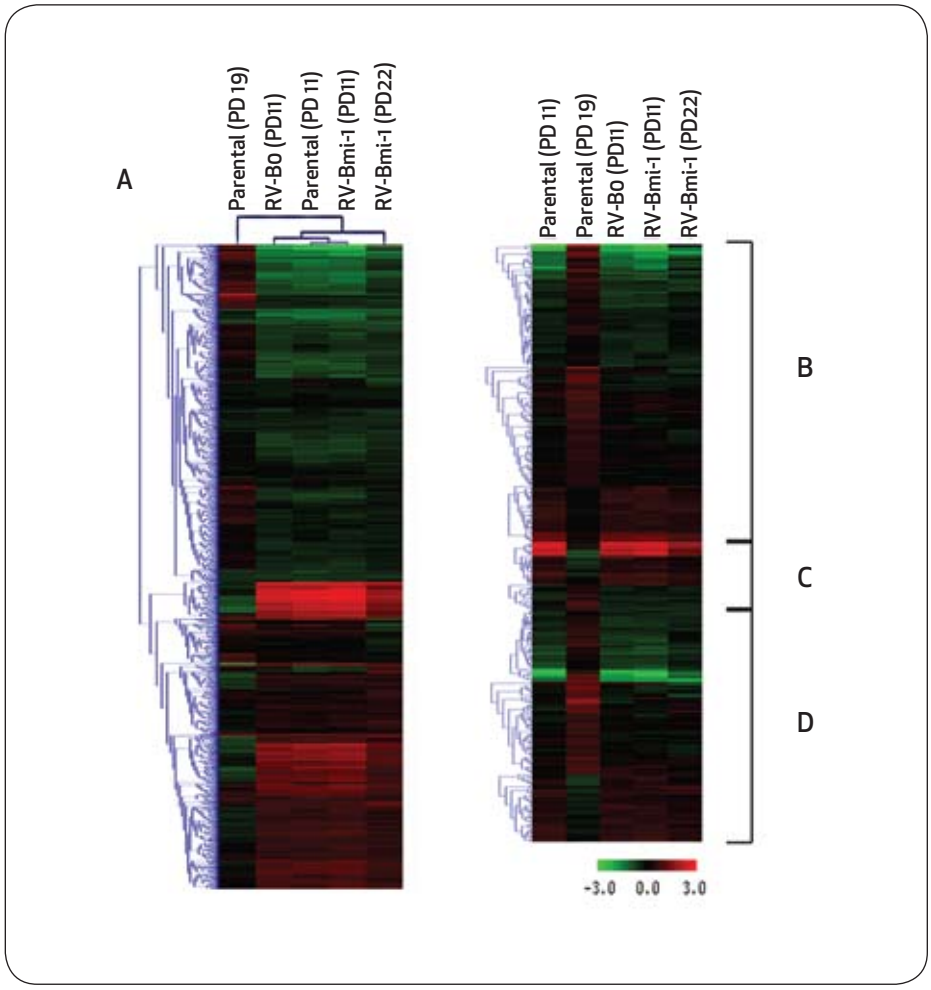

FIGURE 3. Genes are differentially expressed in exponentially replicating NHOK, senescent NHOK, and NHOK with an extended life span. Gene groups and conditions are clustered according to K-means hierarchical clustering statistical algorithms and normalized using RMA normalization with NHOK-RV-Bo (PD 19) as the baseline. Dendrograms display differential expression of 3,024 genes with greater than two-fold change in NHOK-RV-Bo (PD 19) versus NHOK-RV-Bmi-1 (PD 22) (a); genes related to apoptosis (b); genes related to cell cycle arrest (c); and genes related to cellular differentiation (d).

DISCUSSION

The authors reported changes in the gene expression profile of NHOK with an extended life span after ectopic expression of the Bmi-1 oncogene. Of the 47,000 transcripts screened utilizing DNA-microarray in this study, 3,024 transcripts were found to be differentially expressed with greater than two-fold differences. These transcripts reflect the phenotypic differences exhibited between Bmi-1 overexpressing NHOK with an extended life span and senescing late passage NHOK infected with the empty vector control. Expressions of genes involved in cell proliferation, cell differentiation, cell cycle arrest, apoptosis, and senescence were all differentially regulated and profiled.

Of the 3,024 differentially expressed transcripts revealed in this study, there was a clear pattern of recovery when comparing extended-life span, Bmi-1 overexpressing NHOK with senescing NHOK. The global expression pattern of extended-life span, Bmi-1 overexpressing NHOK closely resembled that of exponentially replicating parental NHOK, exponentially replicating empty vector control NHOK, and exponentially replicating Bmi-1 overexpressing NHOK. There was a generally reduced expression of apoptosis related genes in all exponentially replicating NHOK and Bmi-1 overexpressing NHOK with an extended life span, whereas an opposite pattern was exhibited in senescing parental NHOK.

As expected, those apoptosis-related genes typically overexpressed in exponentially replicating NHOK, were also overexpressed in Bmi-1 overexpress-

ing NHOK with an extended life span. However, they were noted to be underexpressed in senescing parental NHOK. This pattern of opposing expression in senescing NHOK, and recovery of expression to exponentially replicating NHOK levels in Bmi-1 overexpressing extended-life span NHOK, was consistent in genes related to cellular differentiation and cell cycle arrest, and was generally present in all of the 3,024 differentially expressed transcripts. These results may indicate that among these genes, there are critical factors that are maintained by Bmi-1-dependent or other mechanisms in exponentially replicating NHOK and are oppositely expressed in senescent NHOK, but may be recovered to their original status by Bmi-1 overexpression in senescent NHOK, resulting in an extended life span.

In a preliminary examination of the differentially expressed genes, the overexpression of Bmi-1 in NHOK/RV-Bmi-1 (PD 22) upregulated several genes related to cell cycle control and cellular proliferation (**TABLE**). The cyclin superfamily, for example, is a group of proteins that are unstable and are subject to rapid turnover. They are responsible for activating cyclin-dependent kinases, which in turn effect progression through the cell cycle, such as through the G1/S-Phase transition.[12] Cyclins A2, B1, E2, and F were all upregulated in Bmi-1 overexpressing NHOK.

Furthermore, another important class of proteins, the cell division cycle (CDC) factors CDC2, CDC6, CDC7, CDC20 and CDC45L were all found to be upregulated in this study. In particular, several of these factors have been suggested to possess oncogenic properties and may be involved in tumorigenesis.[13,14] CDC2 for example, is the catalytic subunit of the M-phase promoting factor complex (MPF), which is essential for the G1/S and G2/M-phase transitions.[15]

CDC2 functions as a kinase that is regulated by cyclin accumulation, and complexes with Cyclin B1 in particular to form MPF, which has also been shown to be upregulated by Bmi-1 in this study. CDC2 has also been shown to complex with Cyclin A and Cyclin E.[16,17] There have been numerous targets of the CDC2/Cyclin complexes documented, and its role in cell-cycle progression and mitosis is widespread. CDC6 has not been as well documented but has been implicated as an important factor in the cell cycle, particularly in DNA replication.[18]

Reports have also shown that CDC6 is regulated by p63 in the initiation of DNA replication, and that aberrant CDC6 expression may be oncogenic in direct repression of the $p^{16INK4A/ARF}$ locus.[19,14] Regulators of cell-cycle progression also comprised several of the upregulated genes, totaling 15. Of particular interest is the minichromosome maintenance deficient (MCM) group of proteins, of which six were upregulated by Bmi-1, and have been well documented in DNA-replication. Interestingly, MCM

TABLE

Differential Expression of Potential Bmi-1 Target Genes

Gene Symbol	Gene Name	Fold Increase (+)/ Decrease(–)
CDC 2	Cell division cycle 2	+2.6
CDC 6	Cell division cycle 6	+3.0
CDC 7	Cell division cycle 7	+2.5
CDC 20	Cell division cycle 20	+2.0
CDC 25A	Cell division cycle 25A	+1.7
CDC 45L	Cell division cycle 45-like	+2.1
Cdk4	Cyclin-dependent kinase 4	+1.4
CCNA2	Cyclin A2	+2.8
CCNB1	Cyclin B1	+2.0
CCND2	Cyclin D2	+1.7
CCNE2	Cyclin E2	+3.0
CCNF	Cyclin F	–2.4
CCNG2	Cyclin G2	–1.7
CCNI	Cyclin I	–1.5
IL1B	Interleukin 1 beta	–1.6
IL8	Interleukin 8	–2.9
MCM 2	minichromosome maintenance complex component 2	+2.6
MCM 3	minichromosome maintenance complex component 3	+1.9
MCM 4	minichromosome maintenance complex component 4	+2.1
MCM 5	minichromosome maintenance complex component 5	+2.6
MCM 6	minichromosome maintenance complex component 6	+5.9
MCM 7	minichromosome maintenance complex component 7	+1.8
MCM 10	minichromosome maintenance complex component 10	+2.6
TGFB2	Transforming growth factor,beta 2	+2.0

2, 4, 6, and 7 form a complex that is phosphorylated by the aforementioned CDC2 and CDC7 kinases.[20]

Overall, several promising avenues of study have been revealed that may further elucidate the physiological mechanisms underlying aberrant Bmi-1 function and its role in oncogenesis. In particular, poorly studied genes and genes with no previously established relationship with Bmi-1 are the most intriguing. Studies are currently being conducted to further validate the data obtained from the microarray analysis, and promising genes are undergoing physiological characterization and functional analysis. Conclusive validation of the role of Bmi-1 in tumorigenesis is also necessitated. In particular, studies involving the tumorigenic potential of Bmi-1 overexpressing NHOK in nude mice would be the most definitive, and would aid in the characterization of the novel genes related to Bmi-1. Taken together, these studies may provide a better understanding of the roles of Bmi-1 and its key factors in cellular transformation and carcinogenesis. ■■■■

REFERENCES

1. Kim RH, Kang MK, et al, Bmi-1 cooperates with human papillomavirus type 16 E6 to immortalize normal human oral keratinocytes. *Exp Cell Res* 313(3):462-72, Feb. 1, 2007.
2. van Lohuizen M, Verbeek S, et al, Identification of cooperating oncogenes in E mu-myc transgenic mice by provirus tagging. *Cell* 65(5):737-52, May 31, 1991.
3. Lessard J, Sauvageau G, Bmi-1 determines the proliferative capacity of normal and leukaemic stem cells. *Nature* 423(6937):255-60, May 15, 2003.
4. Jacobs JJ, Kieboom K, et al, The oncogene and Polycomb-group gene bmi-1 regulates cell proliferation and senescence through the ink4a locus. *Nature* 397(6715):164-8, Jan. 14, 1999.
5. Itahana K, Zou Y, et al, Control of the replicative life span of human fibroblasts by p16 and the polycomb protein Bmi-1. *Mol Cell Biol* 23(1):389-401, 2003.
6. Dimri GP, Martinez JL, et al, The Bmi-1 oncogene induces telomerase activity and immortalizes human mammary epithelial cells. *Cancer Res* 62(16):4736-45, Aug. 15, 2002.
7. Kang MK, Kim RH, et al, Elevated expression of Bmi-1 is associated with dysplastic cell transformation and required for cancer cell replication and survival. *Br J Cancer* 96(1):126-33, Jan. 15, 2007.
8. Kang MK, Bibb C, et al, In vitro replication and differentiation of normal human oral keratinocytes. *Exp Cell Res* 258(2):288-97, Aug. 1, 2000.
9. Kim RH, Christensen R, et al, Elevated expression of hTERT is associated with dysplastic cell transformation during human oral carcinogenesis in situ. *Clin Cancer Res* 7(10):3079-86, October 2001.
10. Friedmann T, Yee JK, Pseudotyped retroviral vectors for studies of human gene therapy. *Nat Med* 1(3):275-7, March 1995.
11. Davis HE, Morgan JR, Yarmush ML, Polybrene increases retrovirus gene transfer efficiency by enhancing receptor-independent virus adsorption on target cell membranes. *Biophys Chem* 97(2-3):159-72, June 2002.
12. Morgan DO, Cyclin-dependent kinases: engines, clocks, and microprocessors. *Annu Rev Cell Dev Biol* 13:261-91, 1997.
13. Murphy N, Ring M, et al, p16INK4A, CDC6, and MCM5: predictive biomarkers in cervical preinvasive neoplasia and cervical cancer. *J Clin Pathol* 58(5):525-34, May 2005.
14. Gonzalez S, Klatt P, et al, Oncogenic activity of Cdc6 through repression of the INK4/ARF locus. *Nature* 440(7084):702-6, March 30, 2006.
15. Dunphy WG, Brizuela L, et al, The Xenopus cdc2 protein is a component of MPF, a cytoplasmic regulator of mitosis. *Cell* 54(3):423-31, July 29, 1988.
16. Draetta G, Luca F, et al, Cdc2 protein kinase is complexed with both cyclin A and B: evidence for proteolytic inactivation of MPF. *Cell* 56(5):829-38, March 10, 1989.
17. Koff A, Cross F, et al, Human cyclin E, a new cyclin that interacts with two members of the CDC2 gene family. *Cell* 66(6):1217-28, Sept. 20, 1991.
18. Yan Z, DeGregori J, et al, Cdc6 is regulated by E2F and is essential for DNA replication in mammalian cells. *Proc Natl Acad Sci USA* 95(7):3603-8, March 31, 1998.
19. Duursma A, Agami R, p53-Dependent regulation of Cdc6 protein stability controls cellular proliferation. *Mol Cell Biol* 25(16):6937-47, August 2005.
20. Hendrickson M, Madine M, et al, Phosphorylation of MCM4 by cdc2 protein kinase inhibits the activity of the minichromosome maintenance complex. *Proc Natl Acad Sci* USA 93(22): pp. 12223-8, October 29, 1996.

TO REQUEST A PRINTED COPY OF THIS ARTICLE, PLEASE CONTACT No-Hee Park, PhD, DMD, dean, University of California, Los Angeles, School of Dentistry, CHS 53-038, 10833 Le Conte Ave., Los Angeles, Calif., 90095.

CDA JOURNAL, VOL 35, Nº12

TGF-β Signaling and Aplasia Cutis Congenita: Proposed Animal Model

ARMEN ZEHNALY; RYOICHI HOSOKAWA, DDS, PHD; MARK URATA, MD, DDS; AND YANG CHAI, DDS, PHD

ABSTRACT TGF-β plays a role in cell migration, proliferation, and differentiation during embryonic development. This study investigated the effect of neural crest- or mesodermspecific loss of TGF-β type II receptor in mice. These conditional knockout mice both exhibit skin defects of the skull associated with an underlying bone defect, a phenotype consistent with the human disorder aplasia cutis congenita. The authors suggest that TGF-β type II receptor gene is a candidate gene for aplasia cutis congenita.

AUTHORS

Armen Zehnaly is a dental student at the University of Southern California School of Dentistry; **Ryoichi Hosokawa, DDS, PhD,** a postdoctoral research associate; and **Mark Urata, MD, DDS,** an assistant professor of oral surgery, are with the Center for Craniofacial Molecular Biology, University of Southern California.

Yang Chai, DDS, PHD, is chair of the Division of Craniofacial Sciences and Therapeutics at the University of Southern California School of Dentistry.

ACKNOWLEDGMENTS

The authors thank Julie Mayo for critical reading of the manuscript and H. Moses and Phil Soriano for the *Tgfbr2*$^{fl/fl}$ and *Myf5-Cre* mice, respectively. This study was supported by grants from the National Institute of Dental and Craniofacial Research, NIH (DE012711, DE014078 and DE017007) to Yang Chai, DDS, PhD.

Congenital syndromic disorders frequently include craniofacial anomalies. For instance, cleft palate, the most common craniofacial disorder, occurs in Treacher-Collins syndrome.[1] The investigation of the etiology of these malformations will hopefully result in the ability to treat and/or prevent these conditions in the future.

Numerous studies have revealed that specific genes are related to particular familiar disorders. In addition, mouse knockout models containing disruptions of genes implicated in human disorders often reproduce the human phenotypes of human. For instance, *Tbx1* null mice exhibit the DiGeorge syndrome phenotype seen in humans with haploinsufficiency of the *TBX1* gene.[2]

Some knockout mice die prematurely at an early developmental stage because of a constitutional defect, such as in vascular system, making it impossible to analyze later developmental events. Therefore, conditional knockout mice have been developed using the Cre-LoxP system.[3] The Cre-Lox system is a powerful tool to control the function of a specific gene in temporal and spatial specific manner. Briefly, the Cre gene is inserted under the regulation of a specific gene promoter and loxP sites are engineered around a gene of interest. When this promoter is activated, Cre protein excises the gene region between the loxP sites. For instance, *Wnt1* is expressed in the neural crest cell lineage during embryonic development and can be used to limit Cre expression temporally and spatially.[3,4]

The authors have previously reported that *Wnt1-Cre;Tgfbr2* lose Transforming Growth Factor-β (TGF-β) signaling in the

neural crest cell lineage, resulting in severe craniofacial defect.[5] TGF-β signaling is involved in important biological functions such as cell migration, proliferation, and differentiation.[6] During embryogenesis, there are two mesenchymal cell lineages in the craniofacial region, cranial neural crest- and mesoderm-derived cells.[7] In this study, the authors analyzed two kinds of conditional knockout mice, lacking TGF-β specifically in their neural crest- or mesoderm-derived cells in order to investigate the contribution of these lineages to craniofacial development. The conditional knockout mice exhibit skin defects of the skull associated with an underlying bone defect.

Aplasia cutis congenital, ACC, is a human disorder characterized by a localized defect of skin structure at birth, usually occurring on the scalp.[8,9] This disorder is frequently complicated by defects of the muscle and bone beneath the affected skin and sometimes associated with a defect of the skull.[10,11] ACC is divided into nine groups.[11] The phenotype of group 4 of ACC, in particular, is very similar to that of both *Myf5-Cre;Tgfbr2*$^{flox/flox}$ and *Wnt1-Cre;Tgfbr2*$^{flox/flox}$ mouse models, suggesting that *Tgfbr2* is a potential candidate gene for ACC.

MATERIALS AND METHODS

All animal studies were performed according to IACUC guidelines.

Two-component Genetic System for Markingthe Progeny of Somite-derived Cells

The *R26R* conditional reporter allele has been described previously.[12] The authors mated *Wnt1-Cre* or *Myf5-Cre* and *R26R* mice to generate *Wnt1-Cre;R26R* or *Myf5-Cre;R26R* embryos. Detection of β-galactosidase activity in whole embryos (Embryonic 9.5 day) was carried out as previously described.[4]

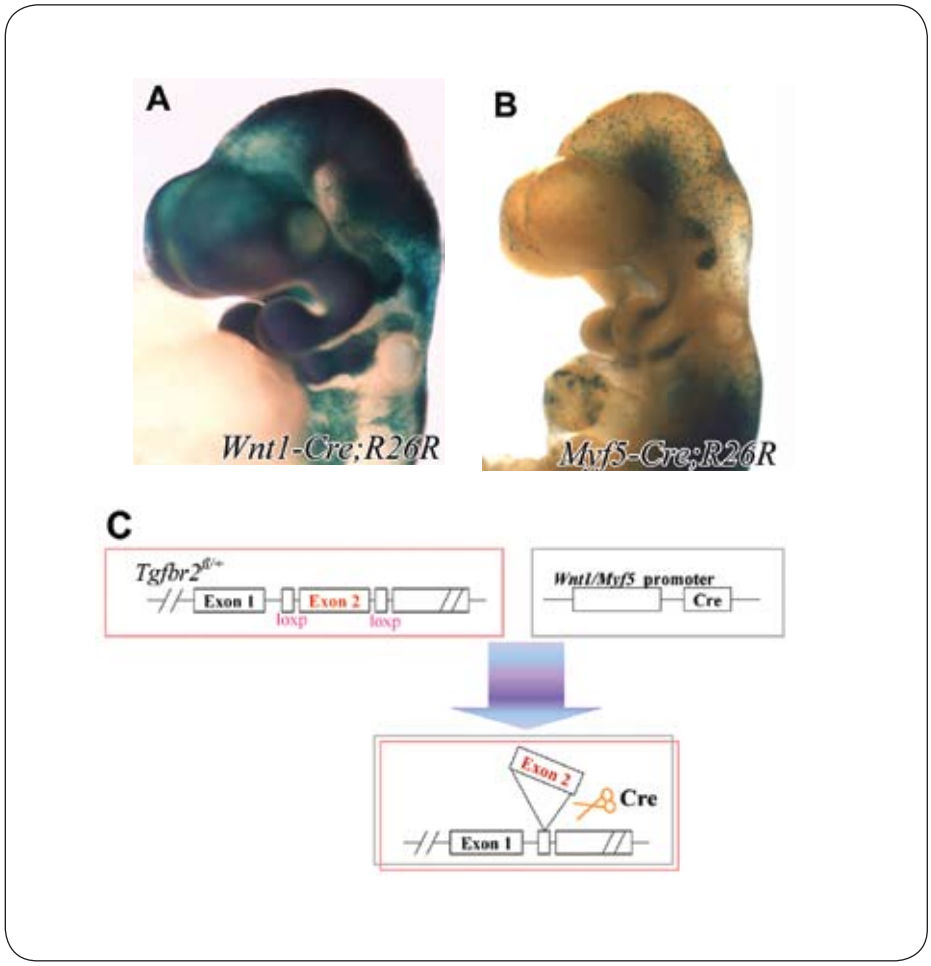

FIGURES 1A-B. Whole mount β-galactosidase activity staining at embryonic day 9.5 of *Wnt1-Cre;R26R* mouse (a) and *Myf5-Cre;R26R* (b) mice. **FIGURE 1C.** Schematic diagram illustrating the conditional knockout mouse strategy.

Generation of *Myf5-Cre;Tgfbr2*$^{flox/Flox}$ Mutant Mice

Wnt1-Cre or *Myf5-Cre* transgenic mice have been described previously.[5,13] The authors crossed *Wnt1-Cre;Tgfbr2*$^{flox/+}$ or *Myf5-Cre;Tgfbr2*$^{flox/+}$ with *Tgfbr2*$^{flox/flox}$ mice to generate *Myf5-Cre;Tgfbr2*$^{flox/flox}$ or *Myf5-Cre;Tgfbr2*$^{flox/flox}$ null alleles that were genotyped using PCR primers as previously described to produce 36 offspring with similar charactersitics.[5]

Staining of Whole Skeleton

Whole skeletal preparations of newborn mice were prepared and stained with Alizarin Red and Alcian Blue as previously described.[14]

RESULTS

Two Mesenchymal Cell Lineages Are Involved in Craniofacial Development

Two cell lineages are involved in craniofacial development: cranial neural crest-derived and mesoderm-derived.[4,7] The Cre-LoxP recombination system is a powerful tool to investigate the fate of specific cell lineages when Cre transgenic mice are crossed with Rosa26R mice.[12] The offspring produce β-galactosidase activity in the Cre expressing cells, which allows the investigator to detect the specific cell lineage. For instance, the neural crest cell lineage can be indelibly marked in *Wnt1-Cre* transgenic mice.[4] At E10.5, cranial neural

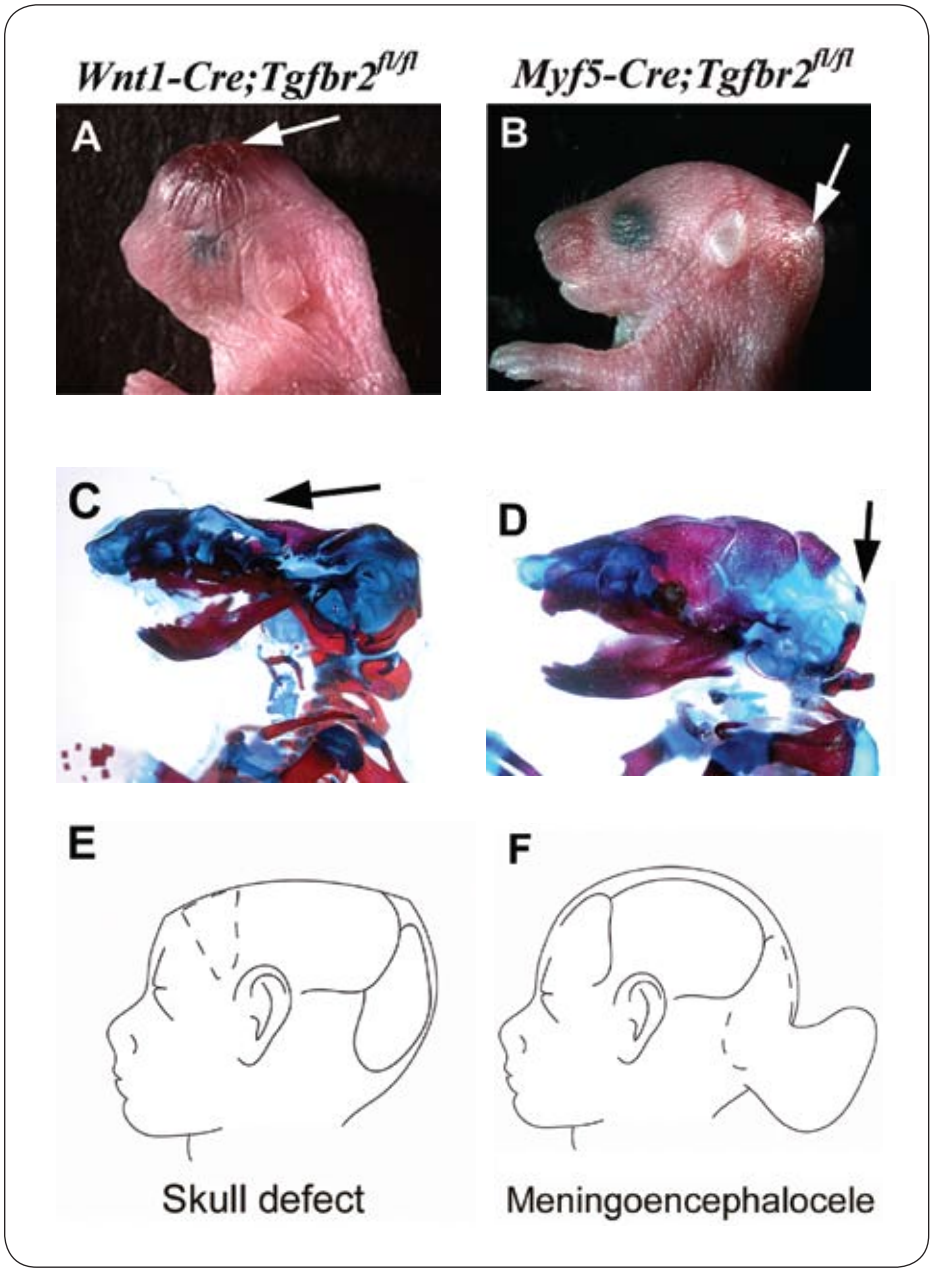

FIGURES 2A-B. Macroscopic appearance of newborn *Wnt1-Cre;Tgfbr2*$^{fl/fl}$ (a) and *Myf5-Cre;Tgfbr2*$^{fl/fl}$ (b) mice. **FIGURES 2C-D**. Alizarin Red and Alcian Blue whole mount bone staining of *Wnt1-Cre;Tgfbr2*$^{fl/fl}$ (c) and *Myf5-Cre;Tgfbr2*$^{fl/fl}$ (d) mice. **FIGURES 2E-F**. Schematic drawing of human patients with frontal bone defect (e) and meningoencephalocele (f).

crest cells populate the branchial arches and front nasal process (blue, **FIGURE 1A**).

Mesenchymal cells are detectable in *Myf5-Cre;R26R* transgenic mice.[13] Mesoderm cells are visible in the core of the branchial arches and somite (blue, **FIGURE 1B**). The blue staining provides a visualization of the cells that will lose TGF-β signaling when Cre transgenic mice are crossed with *Tgfbr2-floxed* mice. **FIGURE 1C** diagrams the authors' strategy for making conditional knockout mice. Cells that express *Wnt1*(cranial neural crest) or *Myf5* (mesoderm) will induce the Cre protein that will excise Exon 2 of the *Tgfbr2* gene. Thus, the creation of Tgfbr2 conditional knockout mice that lack TGF-β specifically in either the cranial neural crest or the mesoderm.

Tgfbr2 Conditional Knockout Mice Exhibit a Defect in Skull Development

Tgfbr2 conventional knockout mice die prematurely at an early embryonic stage.[15] Therefore, the authors made *Tgfbr2* conditional knockout mice specific for the neural crest or the mesoderm.[5,16] *Wnt1-Cre;Tgfbr2*$^{fl/fl}$ mice showed apical swelling and hemorrhage of the head (**FIGURE 2A**, white arrow).

Whole mount bone staining revealed retarded development of the frontal bone (**FIGURE 2C**, black arrow). On the other hand, *Myf5-Cre;Tgfbr2* mice showed swelling and hemorrhage around the occipital area of the head (**FIGURE 2B**, white arrow) and whole mount bone staining revealed a defect of the supraoccipital bone (**FIGURE 2D**, black arrow). These phenotypes of the *Tgfbr2* conditional knockout mice were seen in the human disorder aplasia cutis congenita, such as meningoencephalocele (**FIGURES 2F, E**).

TGF-β Type II Receptor Conditional Knockout Mice Reproduce Phenotypes of Aplasia Cutis Congenita Patients

ACC patients have a congenital skin defect on the skull (**FIGURES 3A, B**). In the few conditional knockout mice that could survive after birth, the authors observed cutis verticis gyrate (**FIGURE 3C**, compared with **FIGURE 3A**, arrows), a phenotype characterized by deep furrows and linear folds on the skin.[17,18] The authors hypothesized that Cre recombination might have occurred in the lateral area without hair, but not in the middle area with hair. To test this hypothesis, the

authors assessed lacZ expression in the skin of *Myf5-Cre;R26R*$^{flox/+}$ mice skin at the newborn stage (**FIGURES 3D, E**). Indeed, hair follicles in the lateral-dorsal area contained only lacZ positive cells (**FIGURE 3E**). In the mid-dorsal area, the hair follicles contained a mixed population of *Myf5-Cre* positive and negative cells (**FIGURE 3D**).

DISCUSSION

The conditional knockout of *Tgfbr2* in mouse neural crest- and mesoderm-derived cells resulted in the disorganization of connective tissue above the defective bone area.[5,16] Aplasia cutis congenital is a rare human congenital skin condition associated with bone and skeletal muscle defects beneath affected skin and is strikingly similar to the phenotype observed in the authors' *Tgfbr2* conditional knockout mouse model (**FIGURE 2, FIGURES 3A-C**). ACC appears to show dominant inheritance but many details remain unknown.[19,20] For instance, one ACC patient has a frontal bone defect associated with a skin defect, but another patient has a parietal bone defect associated with a skin defect.[11,10] ACC is also accompanied by cutis verticis gyrate that is characterized by the appearance of deep, linear skin folds in the scalp[17,18] (**FIGURE 3A**). TGF-β isoforms and TGF-β type II receptor are expressed in hair follicles during embryonic and neonatal stages.[21,22] TGF-β is a critical factor in the formation of connective tissue and promotes the synthesis of extracellular matrix in dermal tissue.[23,24] The cause of the skin defect in our Tgfbr2 mouse model may be the loss of TGF-β signaling in mesenchymal and epithelial cells in hair follicles. These skin structure and hair follicle defects result in a phenotype remarkably similar to ACC. Thus, the authors suggest that *Tgfbr2* is a candidate gene for aplasia cutis congenital. ■■■■

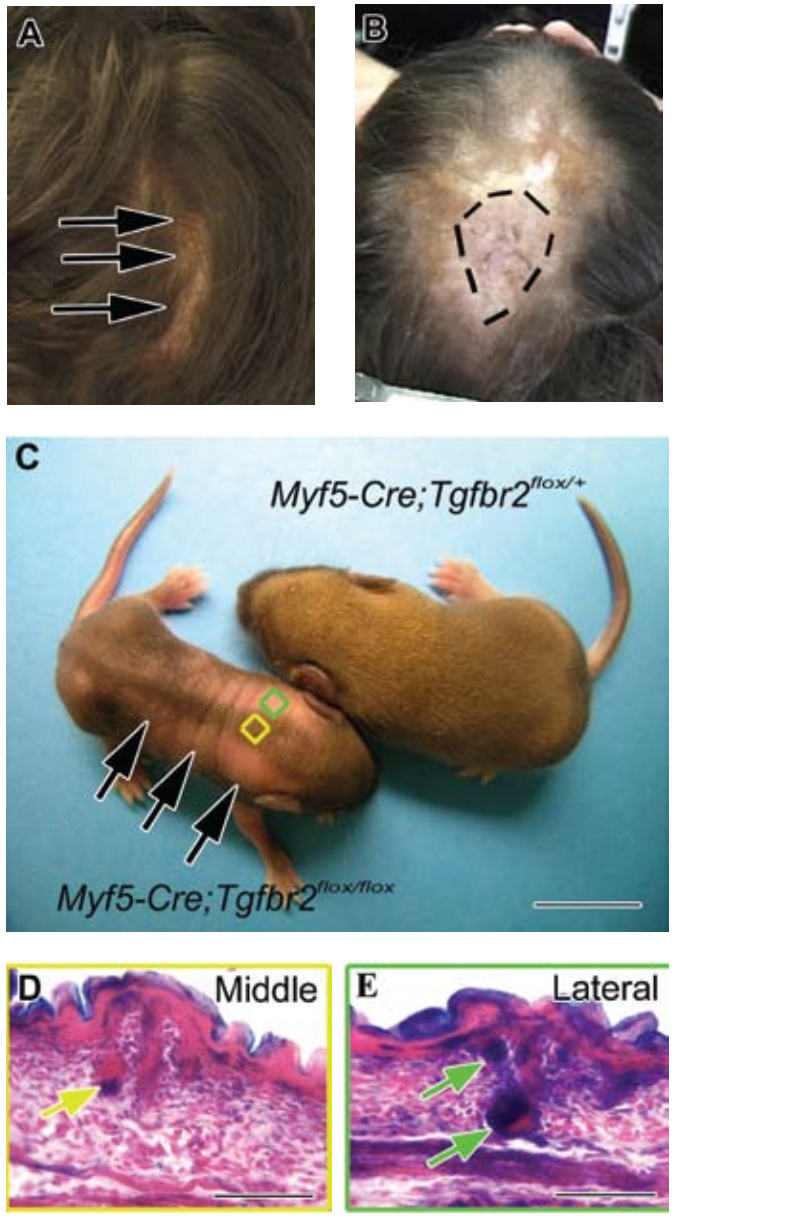

FIGURES 3A-B. Aplasia cutis congenita patients. Arrows indicate cutis vertices gyrate. Dotted circle highlights the congenital skin defect. **FIGURE 3C**. Macroscopic appearance of *Myf5-Cre;Tgfbr2*$^{fl/fl}$ and *Myf5-Cre;Tgfbr2*$^{fl/+}$ mice at postnatal day 10. **FIGURES 3D-E**. Enlarged view of yellow and green boxes in C. Arrows indicate the β-galactosidase activity.

REFERENCES

1. Dixon MJ, Treacher Collins syndrome. *Hum Mol Genet* 5 Spec No., 1391-6, 1996.
2. Jerome LA, Papaioannou VE, DiGeorge syndrome phenotype in mice mutant for the T-box gene, Tbx1. *Nat Genet* 27: 286-91, 2001.
3. Nagy A, Cre recombinase: the universal reagent for genome tailoring. *Genesis* 26, 99-109, 2000.
4. Chai Y, Jiang X, et al, Fate of the mammalian cranial neural crest during tooth and mandibular morphogenesis. *Development* 127, 1671-9, 2000.
5. Ito Y, Yeo JY, et al, Conditional inactivation of Tgfbr2 in cranial neural crest causes cleft palate and calvaria defects. *Development* 130, 5269-80, 2003.
6. Massague J, The transforming growth factor-beta family. *Annu Rev Cell Biol* 6, 597-641, 1990.

7. Noden DM, Interactions and fates of avian craniofacial mesenchyme. *Development* 103 Suppl, 121-40, 1988.
8. Evers ME, Steijlen PM, Hamel BC, Aplasia cutis congenita and associated disorders: an update. *Clin Genet* 47, 295-301, 1995.
9. Kenner JR, Sperling LC, Pathological case of the month. Temporal triangular alopecia and aplasia cutis congenita. *Arch Pediatr Adolesc Med* 152, 1241-2, 1998.
10. Benjamin LT, Trowers AB, Schachner LA, Giant aplasia cutis congenita without associated anomalies. *Pediatr Dermatol* 21, 150-3, 2004.
11. Bonioli E, Hennekam RC, et al, Aplasia cutis congenita, skull defect, brain heterotopia, and intestinal lymphangiectasia. *Am J Med Genet* A 132, 202-5, 2005.
12. Soriano P, Generalized lacZ expression with the ROSA26 Cre reporter strain. *Nat Genet* 21, 70-1, 1999.
13. Tallquist MD, Weismann KE, Hellstrom M, Soriano P, Early myotome specification regulates PDGFA expression and axial skeleton development. *Development* 127, 5059-70, 2000.
14. McLeod MJ, Differential staining of cartilage and bone in whole mouse fetuses by alcian blue and alizarin red S. *Teratology* 22, 299-301, 1980.
15. Oshima M, Oshima H, Taketo MM, TGF-beta receptor type II deficiency results in defects of yolk sac hematopoiesis and vasculogenesis. *Dev Biol* 179, 297-302, 1996.
16. Sasaki T, Ito Y, et al, TGF[beta]-mediated FGF signaling is crucial for regulating cranial neural crest cell proliferation during frontal bone development. *Development* 133, 371-81, 2006.
17. Diven DG, Tanus, T, Raimer SS, Cutis verticis gyrata. *Int J Dermatol* 30, 710-2, 1991.
18. Nguyen NQ, Cutis verticis gyrata. *Dermatol Online J* 9, 32, 2003.
19. Jeannet PY, Watts GD, et al, Craniofacial and cutaneous findings expand the phenotype of hereditary neuralgic amyotrophy. *Neurology* 57, 1963-8, 2001.
20. Jones EM, Hersh JH, Yusk JW, Aplasia cutis congenita, cleft palate, epidermolysis bullosa, and ectrodactyly: a new syndrome? *Pediatr Dermatol* 9, 293-7, 1992.
21. Lawler S, Candia AF, et al, The murine type II TGF-beta receptor has a coincident embryonic expression and binding preference for TGF-beta 1. *Development* 120, 165-75, 1994.
22. Paus R, Cotsarelis G, The biology of hair follicles. *N Engl J Med* 341, 491-7, 1999.
23. Kingsley DM, The TGF-beta superfamily: new members, new receptors, and new genetic tests of function in different organisms. *Genes Dev* 8, 133-46, 1994.
24. Wahl SM, Transforming growth factor beta: the good, the bad, and the ugly. *J Exp Med* 180, 1587-90, 1994.

FOR REQUEST A PRINTED COPY OF THIS ARTICLE, PLEASE CONTACT Armen Zehnaly at zehnaly@usc.edu.

CDA JOURNAL, VOL 35, Nº12

Mighty Mouth

What better way to mark the occasion than pulling a 328-ton train as far as you can with your teeth?

Robert E. Horseman, DDS

ILLUSTRATION BY CHARLIE O. HAYWARD

Does the name Rathakrishnan Velu ring a bell for you? Us neither.

If Anna Chidambar, acting as Rathakrishnan Velu's manager, has her way, his name will be on everyone's lips before the year is out, once they learn to pronounce it. This is not in dentistry's best interests. Should our patients learn of Velu's feat and attempt to emulate it, 90 percent of their dental work will have been for naught.

Here's why: Down in Kuala Lumpur, Malaysia, where he is known as Raja Gigi, or King Tooth, Rathakrishnan is hot stuff. If you had been at the city's railroad station recently as part of the chanting crowd jostling for a better viewpoint with its digital cameras, you would have witnessed history in the making.

King Tooth is standing erect between the rails. Clenched in his mouth is one end of a steel cable about 15 feet long. The other end is attached to a seven-coach train. The enthusiastic crowd is chanting "Malaysia Boleh!" which as near as we can make out, means roughly "Go, idiot!"

King Tooth, wearing a bright orange reflective vest, has one gloved hand to his forehead evoking an Indian form of meditation. This involves a longish period where the mind is banished to some distant point where it can't interfere by offering advice. The chants attain an almost lyrical pitch; King Tooth meditates. He is meditating on Newton's laws of motion, particularly the one that states "a body in motion tends to remain in motion." The trick is to get the motion going in the first place, because he is going to attempt to break his world record set in 2003 by pulling this 328-ton train as far as he can with

CONTINUES ON 909

DR. BOB, CONTINUED FROM 910

his teeth. Apparently his dentist hasn't mentioned a few of the things that could go wrong with this notion, i.e., disengaging his mouth from his face. Informed consent hasn't entered any one's mind at this point, so the stunt remains a focal point of the day's festivities.

Actually, this is more than a stunt. Velu explains to the Bernama News Agency, it is his personal tribute to Merdeka Day, a holiday in Malaysia celebrating the 50th anniversary of its independence from British rule. And what better way to mark the occasion than pulling a 328-ton train as far as you can with your teeth? We can think of a couple, neither of which involves trains or teeth.

In the U.S. we have our share of all-out dare devils. Remember "Nuttier-Than-a-Fruitcake Day" in September 1974 when the alliterative Evel Knievel tried to rocket himself across the Snake River Canyon in Idaho strapped in his Sky-Cycle? The major difference between the two pioneers is that Rathakrishnan actually succeeded in his attempt.

Here's how the *Associated Press* describes the great moment:

"Dozens of onlookers clapped and chanted when Rathakrishnan sat down and pulled the train, holding both tracks for support and pushing his booted feet against the wooden rafters (railroad ties) to propel himself backward."

"Grunting and gasping, Velu's neck muscles strained and his face distorted Thursday as he hauled the nearly 328-ton train over more than 9 feet along tracks at a railroad station in Kuala Lumpur."

Interviewed by reporters after his feat, the Raja Gigi claimed he was disappointed he didn't make his goal of around 14 feet — like that extra 5 feet would have made all the difference. But who's counting? You don't get the title "King Tooth" for nothing in Malaysia.

Nursing his mandible back into position, he declared buoyantly, "I'll be back in December for another try." His main concern seemed to be how long he would be required to suck his curry through a straw.

In the meanwhile, the *Guinness Book of Records* agrees that Rathakrishnan Velu holds the world's record for pulling heavy weights the longest distance with his teeth. Look under "C" for "certifiable weirdoes."

If you have any patients who might wish to share your desire to test the compressive and tensile strength of your restorations and whose IQs test out in the lower 80s, we're sure Amtrak can be persuaded to ante up the train and a length of cable. We could start working on a suitable chant right away. ■■■■